



HAL
open science

Anticipating the fate and impact of organic environmental contaminants: A new approach applied to the pharmaceutical furosemide

Céline Laurencé, Michael Rivard, Thierry Martens, Christophe Morin, Didier Buisson, Sophie Bourcier, Michel Sablier, Mehmet Oturan

► To cite this version:

Céline Laurencé, Michael Rivard, Thierry Martens, Christophe Morin, Didier Buisson, et al.. Anticipating the fate and impact of organic environmental contaminants: A new approach applied to the pharmaceutical furosemide. *Chemosphere*, 2014, 113, pp.193-199. 10.1016/j.chemosphere.2014.05.036 . hal-04049058

HAL Id: hal-04049058

<https://hal.science/hal-04049058>

Submitted on 28 Mar 2023

HAL is a multi-disciplinary open access archive for the deposit and dissemination of scientific research documents, whether they are published or not. The documents may come from teaching and research institutions in France or abroad, or from public or private research centers.

L'archive ouverte pluridisciplinaire **HAL**, est destinée au dépôt et à la diffusion de documents scientifiques de niveau recherche, publiés ou non, émanant des établissements d'enseignement et de recherche français ou étrangers, des laboratoires publics ou privés.

39 **ABSTRACT**

40

41 The presence of trace levels of organic contaminants in the environment is currently an
42 environmental concern. When these contaminants are subjected to environmental
43 transformations, environmental transformation products (ETPs) are obtained, whose
44 structures often remain unknown. The absence of information concerning these new
45 compounds makes them unavailable and consequently makes their environmental detection as
46 well as their (eco)toxicological study impossible. This report describes a multidisciplinary
47 approach that seeks to both anticipate the fate and evaluate the impact of organic
48 environmental contaminants.

49 Our approach consists of three steps. First, isolated and fully characterized transformation
50 products (TPs) of the parent molecule are obtained. This step requires classical organic
51 synthesis and focuses on providing standards of the compounds. In the second step, the parent
52 molecule is subjected to environmentally relevant transformations to identify plausible ETPs.
53 The detection of previously characterized TPs allows the concomitant identification of
54 plausible ETPs. The third step is devoted to the toxicological evaluation of the identified
55 plausible ETPs.

56 Such an approach has recently been applied to furosemide and has allowed the identification
57 of its main TPs. This report now seeks to identify and evaluate toxicologically plausible ETPs
58 of this drug, which is also known as an environmental contaminant.

59

60 Keywords: Furosemide, Electro-Fenton, Bioconversion, Toxicity

61

1. INTRODUCTION

Emerging pollutants are a class of compounds that result from human activity, are detected in the environment and whose impact on ecosystems remains unknown (Levi, 2009). These pollutants consist of compounds that were originally developed as pharmaceuticals and personal care products (PPCPs) (Daughton, 2002; Khetan and Collins, 2007; Fatta-Kassinos et al., 2011a) bactericides or industrial additives (Jurado et al., 2012; Rodil et al., 2012). Regarding the pharmaceuticals, the progress made in trace analysis during the last decade (Buchberger, 2011) has allowed their detection and quantification in the effluents of sewage treatment plants (STPs), rivers, ground water, and sometimes even in drinking water (Heberer, 2002; Kuemmerer, 2004). The presence of pharmaceuticals in the environment mainly occurs after their excretion and results from an incomplete degradation in STPs (Deblonde et al., 2011). Despite their low environmental concentrations, which are generally measured to be less than human therapeutic levels (from ng/L to µg/L), the continuous release of these substances makes them pseudo-persistent, thus presenting a risk of ecotoxicity or chronic toxicity for non-target organisms (Daughton and Ternes, 1999).

Assessing the impact of the presence of drugs (i.e., molecules designed to exert a biological effect) on aquatic biota requires an ecotoxicity or a chronic toxicity to be univocally associated with a perfectly identified chemical structure (or alternatively, to a well-defined mixture of molecules). For this purpose, biological models have been applied to molecules whose presence in the environment had been previously highlighted (Henschel et al., 1997). However, the primary limitation of such studies is that they do not consider the environmental transformation products (ETPs), i.e., compounds stemming from the parent molecule and likely to appear in the environment consecutively to (a)biotic transformations. Attempts to identify ETPs from the analysis of complex environmental matrices, such as soils, sediments or biota, have been demonstrated to be prone to failure (Ibanez et al., 2004; Richardson, 2010). Under these conditions, chromatographic techniques coupled with mass spectrometry in "full-scan" detection mode cannot achieve the detection limits required to characterize these unknown compounds that are present at trace levels. In the absence of characterization, the majority of ETPs remain ill-defined, thus ruling out the evaluation of their (eco)toxicities, which is problematic because the toxicity of ETPs may exceed that of their parent molecules (Dirany et al., 2011; Fatta-Kassinos et al., 2011b; Dirany et al., 2012). In the case of pharmaceuticals, metabolites are a class of ETPs whose structure can be rather well-anticipated (Lohmann and Karst, 2008), and these have already been the subject of

96 environmental detections (Celiz et al., 2009; Mompelat et al., 2009). Further investigations
97 focusing on the identification of new ETPs and the assessment of their impact has led to the
98 development of various strategies (Escher and Fenner, 2011). With this aim, experiments that
99 mimic the transformations that drugs undergo in the environment have been developed
100 (Ziylan and Ince, 2011). These experiments, which were applied to the parent molecule,
101 resulted in transformation products (TPs) assumed to be real (at least similar to) ETPs. Such
102 experiments typically proceed by electro-Fenton (Oturán et al., 1999), photodegradation
103 (Packer et al., 2003) or biodegradation (Ericson, 2010; Gauthier et al., 2010). Because of such
104 protocols and thanks to the means now available, elucidating the structure of these
105 compounds is possible. Nevertheless, authentication of the structure requires the use of
106 standards either commercially available or synthesized (Schulze et al., 2010; Svanfelt and
107 Kronberg, 2011). In the absence of isolated compounds, (eco)toxicological studies are
108 conducted on mixtures of TPs resulting from the degradation of the parent molecule.
109 Interestingly, examples of (eco)toxicological evaluations of fully characterized TPs obtained
110 and isolated after the degradation of the parent pharmaceutical remain scarce (Isidori et al.,
111 2006).

112 In this report, we describe a new approach that enables both the identification of plausible
113 ETPs and their toxicological evaluation. Because the main difficulty in studying the fate of
114 drugs in the environment lies in the lack of authentic samples of their ETPs, we propose a
115 new stepped approach. The first step consists of isolating the TPs of a drug that is known to
116 be an environmental contaminant. This step, which requires the tools of organic synthesis,
117 focuses on providing fully characterized standards and the development of methods for their
118 detection in complex mixtures. In the second step, the contaminant is submitted to
119 environmentally relevant transformations, i.e., processes that are representative of the
120 transformations undergone by contaminants in the environment. By highlighting previously
121 characterized TPs, this step allows the identification of plausible ETPs. In the third step, a
122 toxicological study is initiated on each of the TPs that are identified as plausible ETPs.

123 In a recent work, we described the behavior of furosemide **1** (fig 1) under oxidative
124 conditions (Laurence et al., 2011). This drug, which has been widely used as a diuretic since
125 the nineteen sixties, is one of the forty compounds having the highest risk with a predicted
126 environmental concentration greater than 100 ng/L (Besse and Garric, 2008). Poorly
127 metabolized and eliminated either unmodified or as glucuronide conjugate (Lee et al., 1997)
128 (which releases furosemide after hydrolysis), this drug has been detected at concentration
129 ranges between 61 and 200 ng/L in European rivers (Castiglioni et al., 2006; Khalaf et al.,

130 2009). During the course of our preliminary study, three TPs of furosemide were identified:
131 furfural **2**, saluamine **3** (both resulting from the oxidation of the amino group) and a
132 zwitterionic pyridinium **4** (resulting from the oxidation of the furan ring). These three TPs,
133 which are obtained by anodic oxidation, have been isolated and fully characterized, thereby
134 allowing their detection by LC-MS in complex mixtures.

135 This study seeks to confirm whether these three TPs, which were obtained without any
136 environmental relevance, are indeed plausible ETPs. For this purpose, environmentally
137 relevant degradation pathways were applied to furosemide. To be representative of the
138 transformations likely to occur in the environment, two protocols were selected. The first
139 protocol is abiotic and uses an electrochemical advanced oxidation process (electro-Fenton);
140 the second protocol is biotic and requires microorganisms. The TPs identified as plausible
141 ETPs were then subjected to a preliminary toxicological study.

142

143 **2. MATERIAL AND METHODS**

144

145 **2.1 Chemicals**

146

147 Furosemide (> 99.0%) was purchased from TCI Europe N.V. Furfural (99%) and 1-Methyl-
148 4-phenylpyridinium iodide (MPP⁺) were purchased from Sigma-Aldrich. Saluamine **3** and
149 pyridinium **4** employed for the toxicological evaluation and required as standards for the
150 analysis of complex mixtures were prepared as previously described (Laurence et al., 2011).
151 Dulbecco's Minimal Essential Medium (DMEM), fetal bovine serum (FBS),
152 penicillin/streptomycin, trypsin-EDTA solution and phosphate buffered saline (PBS) were
153 purchased from GibcoBRL (France). The caspase fluorogenic substrate N-Acetyl-Asp-Glu-
154 Val-Asp-7-amido-4-trifluoromethylcoumarin (Ac-DEVD-AFC) was purchased from
155 Calbiochem (France). Sodium chloride (NaCl), 4-(2-hydroxyethyl)-1-
156 piperazineethanesulfonic acid (HEPES), triton X-100, dithiothreitol (DTT), and 3-(4,5-
157 dimethylthiazol-2-yl)-2,5-diphenyltetrazolium bromide (MTT) were purchased from Sigma-
158 Aldrich (Germany).

159

160 **2.2 Analytical procedure**

161

162 ESI-MS/MS analyses were conducted using a Q-TOF Premier instrument equipped with
163 a Z-spray electrospray source (Waters, Saint Quentin-en-Yvelines, France) operating in the
164 positive mode. For fragmentation studies, solutions were introduced into the electrospray
165 ionization source using a syringe pump at an infusion rate of 10 $\mu\text{L}/\text{min}$. To investigate the
166 degradation products, the sample was analyzed using a 2690 liquid chromatography module
167 from Waters (Saint Quentin-en-Yvelines, France) coupled with a Q-TOF premier mass
168 spectrometer. The employed analytical column was a C18 Atlantis T3, 3 μm , 150 x 2.1 mm
169 (Waters, Saint Quentin-en-Yvelines, France). The HPLC solvents were acetonitrile with 0.1%
170 formic acid (A) and water with 0.1% formic acid (B). The following linear gradient elution
171 program was applied: 20% of A for 11 min and 100% of A from 11.1 to 20 min. Then, before
172 the next injection cycle, the column was reconditioned with 20% of A for 10 min. The
173 effluent was introduced at a rate of 0.2 mL/min into the Z-spray interface for ionization. The
174 following three acquisition modes were used to characterize each compound: (i) full-scan
175 mode in V-mode; (ii) MS/MS of the precursor ion and (iii) full-scan in the W-mode for high
176 resolution. The full-scan acquisition mode allowed the cone voltage to be optimized to obtain
177 maximum intensity for the precursor ion. Several MS/MS spectra were recorded to obtain the
178 decomposition pathways.

179 The cone voltage was adjusted for each ion of interest that was generated in the ion
180 source. The ion source parameters were adjusted as follows to optimize the ion signals: the
181 cone voltage was set between 20 to 80 V while the capillary voltage was set to 2.6 kV.
182 Typical values for the other source parameters were as follows: extraction cone, 1.7 V; ion
183 guide, 3 V; source and desolvation temperatures were set at 80 $^{\circ}\text{C}$ and 250 $^{\circ}\text{C}$ for direct
184 infusion and at 100 $^{\circ}\text{C}$ and 450 $^{\circ}\text{C}$ for LC-MS studies, respectively. Nitrogen was used as
185 both nebulizing and desolvation gases. The gas flow rates were dependent on the introduction
186 mode; they ranged from 20 L/h to 300 L/h for direct introduction and from 70 L/h to 700 L/h
187 for LC-MS. For LC-MS analysis, the injected volume of sample was 10 μL . Argon was used
188 as a collision gas at a flow of 0.28 mL/min, which corresponds to a pressure of ca. $4 \cdot 10^{-3}$
189 mbar. To record the MS/MS spectra of ions, the collision energies were varied between 2 to
190 30 eV for each compound to obtain their primary characteristic ions. For accurate mass
191 measurements, the analyses were performed using W-mode and an independent reference
192 spray via the LockSpray interface. Sulfadimethoxine was used as the lock mass compound at
193 a flow rate of 10 $\mu\text{L}/\text{min}$. The LockSpray frequency was set at 10 s, and data for the reference
194 compounds were averaged over 10 spectra/min. Accurate masses and elemental compositions

195 for all ions were obtained using the MassLynx instrument software. The ion used for the mass
196 correction was m/z 311.0814.

197

198 **2.3 Electro-Fenton**

199

200 Experiments were conducted in an open, cylindrical and undivided glass cell of 6 cm
201 diameter and 250 mL capacity. This cell was equipped with a cylindrical Pt mesh (4.5 cm
202 height, 3.1 cm internal diameter) as an anode and a large surface area (14 cm x 4.5 cm each
203 side, 0.5 cm width) carbon felt (Carbon-Lorraine, France) as a cathode. The anode was
204 centered in the electrochemical cell and surrounded by the cathode, which covered the inner
205 wall of the cell. Electrolyses were conducted under a constant current applied by a Hameg
206 HM8040 triple power supply. H₂O₂ was produced from the reduction of O₂ dissolved in the
207 solution. Continuous saturation of this gas at atmospheric pressure was ensured by bubbling
208 compressed air. 220 mL of solutions containing 0.1 to 0.3 mM furosemide and 0.5 mM Fe²⁺
209 at the optimum pH value of 3.0 were electrolyzed at a constant current (30-350 mA) at room
210 temperature. The decrease in the concentration of furosemide and the formation of oxidation
211 intermediates were followed using a Merck Lachrom HPLC chromatograph composed of a
212 degasser (L-7614), an injection pump (L-7100 equipped with a 20 µL injection loop), a
213 reverse phase RP-18 Purospher column (5 µm, 4.6 mm× 25 cm) placed into a L-7350 oven set
214 to 40 °C and a photodiode array detector (L-4755) selected at 280 nm. The mobile phase
215 consisted of a mixture of methanol and phosphoric acid (55/45 (v/v)) at a pH of 3. Elution
216 was performed in isocratic mode with a flow rate of 0.7 mL/min. Identification of aromatic
217 intermediates was conducted by comparing the retention times with that of authentic
218 compounds and UV-Vis spectra. The analyses were monitored using the EZChrom Elite
219 software package.

220

221 **2.4 Bioconversion**

222

223 Microorganisms, including 48 fungi and 24 bacteria, were cultured in liquid medium (25
224 mL) containing in g/L: yeast extract (Conda) 4, malt extract (Conda) 10, soybean peptones
225 (OrganoTechnie) 5, and glucose 16. The process of selection involved six series of 12
226 microorganisms. After sufficient growth, the biomasses were harvested by centrifugation
227 (bacteria) or filtration (fungi) and suspended in 12 mL of a 0.1 M sodium citrate buffer (pH
228 5). For each series, four incubation mixtures (3 fungi and 2 bacteria) were created using the

229 suspensions (4 mL, total volume of 20 mL). Furosemide was dissolved in *N,N*-
230 dimethylformamide (0.066 mg/ μ L) and 60 μ L of this solution were added to the incubation
231 mixtures (final concentration 0.2 mg/ml). Biotransformations were performed under an air
232 atmosphere at 27 °C and 200 rpm and monitored by HPLC and MS. Aliquots (culture medium
233 and biomass; 0.8 mL) were withdrawn every two days, diluted with methanol (200 μ L),
234 mixed vigorously and centrifuged at 13,000 g for 5 minutes. The resulting supernatants were
235 micro-filtered (0.45 μ m) before analysis.

236

237 **2.5 Toxicity measurements**

238

239 *2.5.1 MTT Cell Viability Assay*

240

241 Human neuroblastoma cells (SH-SY5Y) (ATCC CRL2266) were cultured in DMEM (in 75
242 mL flasks), containing 4.5 g/L glucose and supplemented with 1% penicillin/streptomycin and
243 10% FBS, at 37 °C in a humidified atmosphere of 5% CO₂. Cell viability was measured using
244 the MTT assay in 96-well plates at a cell density of 8×10^4 cells/mL. The cells were exposed
245 to different compounds (**1**, furfural **2**, **3** and **4**) at various concentrations (from 1 to 1000 μ M).
246 All drugs were dissolved in a mixture of DMSO and DMEM (1/1 (v/v)) in order to obtain a
247 10^{-1} M stock solution. All controls were carried out using the same solvent mixture. The final
248 solution contained no more than 0.5% (v/v) of DMSO. After 24, 48, 72 and 96 h of exposure,
249 MTT (20 μ L, 5 mg/mL) was added to each well. Following incubation at 37 °C for 2 h, the
250 supernatants were carefully removed and 200 μ L of DMSO were added. The optical density
251 (OD) value of each well was read using a micro-plate reader (TECAN Infinite M1000) at a
252 wavelength of 570 nm. Cell viability was calculated as a percentage of the control.

253

254 *2.5.2 Caspase-3 activity*

255

256 The caspase-3 activity was assessed by following the cleavage of the fluorogenic
257 substrates Ac-DEVD-AFC. Treated cells were harvested through trypsinization using 0.05%
258 trypsin and 0.53 mM EDTA at 37 °C in a humidified atmosphere containing 5% CO₂ for 4
259 min. Trypsinization was terminated by addition of 20% FBS, the cell suspension was then
260 centrifuged, the supernatant discarded and the pellet washed with $1 \times$ PBS (CaCl₂-, MgCl₂-
261 free) (Gibco, Invitrogen). The cell pellet was gently suspended in a buffer containing 30 mM

262 HEPES, 0.3 mM EDTA, 100 mM NaCl, 0.15% Triton X-100 and 10 mM DTT and then
263 centrifuged. The supernatant was used for the assay. The fluorogenic substrates were added at
264 a final concentration of 100 mM. The samples were gently mixed and incubated in the dark at
265 37 °C for 1 h. Fluorescence intensity of the samples was measured at an excitation λ of 400
266 nm and emission λ of 505 nm using a fluorescence micro-plate reader (TECAN infinite™
267 M1000).

268

269 2.5.4 Data analysis

270

271 Data were expressed as the mean \pm SEM. Comparisons among groups were conducted
272 using an ANOVA (F-test) test. Bonferroni adjusted t-tests were used for multiple group
273 comparisons and the unpaired t-test was used for single comparisons. A two-tailed $p < 0.05$
274 was selected to indicate a statistically significant difference. All values were calculated using
275 the GraphPad Prism 5.00 software package (GraphPad Software, San Diego, CA).

276

277 3. RESULTS

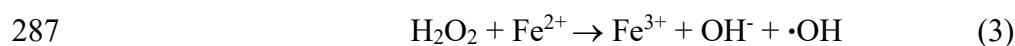
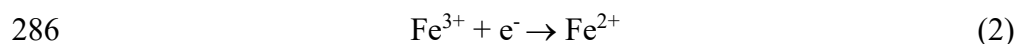
278

279 3.1 Electro-Fenton

280

281 In the first step, furosemide was subjected to electro-Fenton oxidative degradation. This
282 method is based on the *in situ* and catalytic production of hydroxyl radicals ($\cdot\text{OH}$) from the
283 electrochemically assisted Fenton's reaction (Eqs. 1-3).

284

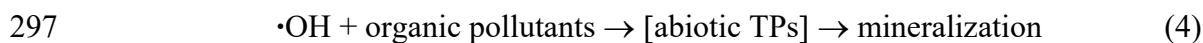


288

289 The hydroxyl radical is a very powerful oxidizing agent, and it non-selectively reacts
290 with organic molecules to lead to the formation of abiotic TPs. In the treatment strategy, the
291 operating parameters were established to further oxidize these intermediates until they
292 reached their ultimate degree of oxidation, i.e., their mineralization (Eq. 4) (Oturán et al.,
293 2000; Sires et al., 2007; Brillas et al., 2009). This process has been successfully applied for

294 the treatment of toxic/persistent pollutants and particularly for the removal of pharmaceutical
295 pollutants from water (Ozcan et al., 2008; Dirany et al., 2010; Sires et al., 2010).

296



298

299 As stated above, the electro-Fenton process was used to mimic the abiotic
300 transformations that are likely to occur in the environment. Contrary to the abatement
301 (treatment) strategy, the inhibition of oxidation kinetics was consequently required to allow
302 the accumulation of the abiotic TPs. Briefly, this inhibition consisted of applying a small
303 current (for weakening the rate of Eqs. 1 and 2) and using a high concentration of catalyst
304 (Fe^{2+}) to favor the waste reaction between $\cdot\text{OH}$ and Fe^{2+} (Eq. 5), thus lowering the
305 concentration of $\cdot\text{OH}$ and consequently the oxidation rate of the intermediates.

306



308

309 This strategy was applied under a pH of 3 at room temperature to a 230 mL aqueous
310 solution of furosemide (0.3 mM) using a current of 50 mA between a Pt anode and a carbon-
311 felt cathode in the presence of Fe^{2+} (0.5 mM) as a catalyst. After 5 min of electrolysis, HPLC
312 analysis of an aliquot revealed the presence of several abiotic TPs. Preparative
313 chromatography on an RP 18 column allowed the isolation of the main compound and its
314 characterization by $^1\text{H-NMR}$. After comparison with the previously obtained data, the aniline
315 derivative **3** (Fig 1) was unambiguously identified. The co-product of this oxidation process,
316 the furfural, was also identified among the other abiotic TPs by comparison with the HPLC
317 chromatogram and UV spectrum of an authentic sample.

318 Monitoring the electro-Fenton treatment of furosemide by HPLC and analyzing aliquots
319 by LC-MS confirmed the formation of compound **3** with the presence of the m/z 251
320 protonated molecular ion (see SI §2). Two other compounds with protonated molecular ions
321 at m/z 329 and m/z 345 were also observed. The structure associated with m/z 329 was
322 confirmed by comparison with previously obtained data and unambiguously identified as
323 pyridinium **4** (see SI §4). The CID mass spectrum analysis led to the proposal of structure **A**
324 (see SI §5, 6) for m/z 345 (Fig 2a).

325 To identify further oxidation products of furosemide, electro-Fenton oxidation was
326 performed on pyridinium **4**. Under these conditions, the compound previously associated with

327 structure **A** was again observed (see SI §5) as well as the aniline derivative **3** (see SI §3). The
328 oxidation of the pyridinium ring of **4**, which leads to intermediates such as **A**, may explain the
329 formation of the latter. Meanwhile, LC-MS analysis of the reaction mixture allowed the
330 observation of two compounds with pseudo-molecular ions at m/z 317 and 282 for which
331 structures **B1** and **C1** (Fig 2b) have been, respectively proposed (see SI §7-10). The same
332 experiment also revealed the presence of two isomers of **B1** and **C1**. The analysis of the CID
333 mass spectra did not allow their univocal characterization, which leads to the proposal of the
334 regioisomers **B2** or **B3** for m/z 317 and **C2** or **C3** for m/z 282.

335

336 **3.2 Bioconversion**

337

338 Furosemide is poorly metabolized by humans; however, this does not exclude the
339 possibility for non-target organisms disposing of the appropriate enzymatic equipment to
340 achieve the transformation of furosemide. One way to fairly accurately identify the spectrum
341 of biotic TPs arising from furosemide consists of subjecting this molecule to microbial
342 transformation (bioconversion). The enzymes that are present in many microbial strains allow
343 access to a wide range of biotransformation products. This approach, which is especially used
344 in the preparation of mammalian metabolites (Smith and Rosazza, 1975; Azerad, 1999; Asha
345 and Vidyavathi, 2009), requires the selection of active microorganisms (Li et al., 2008;
346 Marvalin and Azerad, 2011).

347 To obtain the biotic TPs of furosemide, a selection of microorganisms among seventy-
348 two strains of bacteria and fungi was performed. To complete the screening using minimal
349 time and assays, we used our recently developed combinatorial approach (Fromentin et al.,
350 2012; Joyeau et al., 2013). This method is based on incubating the substrate in the presence of
351 five microorganisms (three fungi and two bacteria) in a reaction buffer. After furosemide was
352 added to the suspensions, the biotransformations were monitored by HPLC and MS analyses
353 of aliquots collected every forty-eight hours.

354 This strategy allowed identification of four microorganisms capable of performing the
355 biotransformation of furosemide as well as the observation of two major biotic TPs.
356 Saluamine **3**, which resulted from the hydrolysis of the intermediate hemiaminal, was
357 obtained with a yield of 25-30% after four days of incubation with the bacteria *Agrobacterium*
358 *tumefaciens* (*Rhizobium radiobacter* CIP 67.1) and *Arthrobacter ureafaciens* CIP 67.3. This
359 result confirmed the ability of the microorganisms to oxidize the α -position of the amino
360 group of furosemide, as previously observed (Hezari and Davis, 1992). The absence of

361 furfural may be explained by the ability of some microorganisms to degrade it (Koopman et
362 al., 2010). The fungus *Aspergillus candidus* ATCC 20023 produced pyridinium **4** in moderate
363 yields after eight days (see SI §4). The fungus *Cunninghamella echinulata* var. *elegans* ATCC
364 9245 fully metabolized furosemide in six days to yield a mixture of both compounds. In some
365 cases, the compound associated with structure **A** was also observed as a minor biotic TP (see
366 SI §5). Further investigations are in progress to optimize the production of this TP to isolate it
367 and confirm its structure.

368

369 **3.3 Toxicological evaluation of plausible ETPs**

370

371 The evaluation on the neuroblastoma cell line (SH-SY5Y) of furosemide **1** revealed no
372 activity on the tested cells after 24 and 48 h. However, after 72 h, a slight inhibition of
373 approximately 20% of the cell survival was observed, which is possibly explained by the
374 action of furosemide on the regulation of the cytosolic pH (Rakonczay et al., 2008). An
375 extended exposure to furosemide for 96 h did not reveal any increased inhibition.

376 In the same test, the saluamine **3** was completely inactive up to 96 h at all investigated
377 concentrations. Exhibiting no toxicity after 24 and 48 h, furfural **2** reduced the cell viability
378 by approximately 20% after 72 h at the maximal concentration of 1000 μM . As observed with
379 the furosemide, no increased inhibition was observed after extended exposure. Interestingly,
380 pyridinium **4** also began to have an effect after 72 h of exposure. The effect of pyridinium **4**
381 on the cell mortality was increased from 40 to 60% between 72 to 96 h. The concentration at
382 which 50% of the cells survived (EC_{50}) was estimated to be 973 μM (Fig 3a).

383 The induction of cell death by exposure to pyridinium **4** was confirmed after evaluation
384 of the caspase-3 activity (Fig 3b). The increased activity (175%) observed after 96 h for the
385 treated cells compared to the untreated ones (100%) allowed the previously observed cell
386 death to be clearly associated with an apoptotic process.

387

388 **4. DISCUSSION**

389

390 Anticipating the fate of emerging pollutants often leads to complexity in investigating
391 and researching ETPs, which for the most part remain unknown. By detecting after
392 degradation of a contaminant by environmentally relevant transformations, compounds that
393 have been fully characterized in a previous step, our approach has demonstrated its ability to
394 univocally identify plausible ETPs of organic pollutants. Interestingly, the alternative

395 approach consisting of applying environmentally relevant transformations to a contaminant to
396 obtain, isolate and characterize its plausible ETPs in a single step might seem intuitively
397 quicker and more appropriate. However, the results of this study suggest that such an
398 approach would have failed to detect plausible ETPs exhibiting significantly different
399 physicochemical properties from those of the parent compound, as in the case of pyridinium
400 **4**. Note that saluamine **3** has already been identified as a biotic TP of furosemide after
401 bioconversion with the fungus *Cunninghamella elegans* (Hezari and Davis, 1992). The fact
402 that pyridinium **4** was not observed in the same study may be explained by the unavailability
403 of any standard. However, Burka observed the formation of pyridinium **4** after the liver
404 microsomal incubation of furosemide (Chen and Burka, 2007), but this was consecutive to its
405 NMR characterization after the oxidation of furosemide with dimethyldioxirane in deuterated
406 acetone.

407 Because electro-Fenton degradation and bioconversion are representative of the
408 transformations that are likely to occur in the environment, the saluamine **3** and the
409 pyridinium **4**, which both result from these two degradation processes, can consequently be
410 considered as plausible ETPs of furosemide. With the help of available standards, the
411 implementation of protocols for the environmental detection of these ETPs can now be
412 initiated. A possible co-product of the oxidation leading to aniline **3**, furfural, is therefore also
413 a plausible ETPs of furosemide. The abundant use of this compound stemming from the
414 biomass for industrial purposes makes it nevertheless an unreliable marker of the presence of
415 furosemide in the environment. Additionally, while the growth-inhibiting properties of
416 furfural have already been mentioned (Almeida et al., 2009), it appears that the concentrations
417 at which furosemide is detected in the environment make the risk associated to its ability to
418 release furfural not significant (Wierckx et al., 2011).

419 By the observation of compounds **A**, **B** or **C** and the collection of their analytical data,
420 our approach has also allowed the identification of new plausible ETPs, including their
421 detection in any complex mixtures. To complete their characterization, their structure
422 proposed on the basis of CID mass spectrum analysis and structural similarities with provided
423 standards, has to be confirmed or refined (which is why they were indicated with letters, not
424 numbers). This confirmation process requires either their isolation from degradation mixtures
425 or their total synthesis (this work is currently underway). Note that each new compound that
426 is isolated and authenticated as a plausible ETP can be subsequently subjected to
427 environmentally relevant transformations and toxicologically evaluated. Such iterative
428 protocol appears appropriate to anticipate further oxidation states of contaminants and thus, to

429 accurately predict their environmental fate, either on a structural or on a toxicological basis.
430 Interestingly, anticipating such further oxidation states of contaminants allowed the
431 environmental fate of furosemide to be reconsidered. Indeed, whereas the anodic oxidation,
432 which is focused on the earlier oxidation states, suggested the aforementioned two distinct
433 degradation pathways (proceeding by oxidation of either the amino group or the furan ring),
434 this study revealed the ability of **4** to release saluamine **3** after over-oxidation of its
435 pyridinium ring. Such information may be of interest for investigating the kinetics of the
436 appearance and disappearance of toxicity associated with the transformation of contaminants
437 in the environment.

438 The final part of this study was devoted to the toxicological evaluation of plausible ETPs,
439 and it highlighted the difference in terms of toxicity between the parent molecules and their
440 ETPs. The present study has consequently confirmed the necessity of developing new
441 methodologies to anticipate the fate of environmental contaminants. Furthermore, this study
442 has also demonstrated the need to provide suitable samples for biological tests, i.e., obtained
443 on preparative scale and isolated. This latter point was demonstrated to be crucial for
444 univocally associating toxicity to a chemical structure. In the case of furosemide, note that if a
445 genotoxicity has already been mentioned, no molecule has yet been clearly associated with it
446 (Rocco et al., 2010; Mondal et al., 2012). To date, only a reactive intermediate in the form of
447 an epoxide has been proposed to explain the cytotoxicity of this drug (Williams et al., 2007).
448 The present work may consequently help the mechanism for the toxicity of furosemide to be
449 reconsidered in relation with one of its TPs.

450 In summary, our multidisciplinary approach for anticipating the fate of environmental
451 contaminants allowed identifying three plausible ETPs of furosemide, and five other ETPs
452 were observed whose chemical structures must be confirmed or refined. The availability of
453 standards now enables the environmental investigations and, possibly, the quantification of
454 aniline **3** and pyridinium **4**, which appear as relevant markers of the presence of furosemide in
455 the environment.

456 The biological results also revealed a significant toxicity for the pyridinium **4**. Following this
457 work, assessment of the risk associated with the presence of furosemide in the environment
458 requires a particular focus on this plausible ETP, whose mechanism of action remains
459 unknown and whose ecotoxicity remains to be investigated.

460

461 **5. ACKNOWLEDGMENTS**

462

463 We thank the CNRS for funding (CPDD), MESR for a PhD fellowship and Caroline Bance
464 for technical support in microbiology.
465

466

467 Almeida JRM, Bertilsson M, Gorwa-Grauslund MF, Gorsich S and Liden G (2009) Metabolic
468 effects of furaldehydes and impacts on biotechnological processes. *Appl. Microbiol.*
469 *Biotechnol.* **82**:625-638.

470 Asha S and Vidyavathi M (2009) Cunninghamella - A microbial model for drug metabolism
471 studies - A review. *Biotechnol. Adv.* **27**:16-29.

472 Azerad R (1999) Microbial models for drug metabolism. *Adv. Biochem. Eng./Biotechnol.*
473 **63**:169-218.

474 Besse J-P and Garric J (2008) Human pharmaceuticals in surface waters. *Toxicol. Lett.*
475 **176**:104-123.

476 Brillas E, Sires I and Oturan MA (2009) Electro-Fenton Process and Related Electrochemical
477 Technologies Based on Fenton's Reaction Chemistry. *Chem. Rev. (Washington, DC,*
478 *U. S.)* **109**:6570-6631.

479 Buchberger WW (2011) Current approaches to trace analysis of pharmaceuticals and personal
480 care products in the environment. *J. Chromatogr. A* **1218**:603-618.

481 Castiglioni S, Bagnati R, Fanelli R, Pomati F, Calamari D and Zuccato E (2006) Removal of
482 Pharmaceuticals in Sewage Treatment Plants in Italy. *Environ. Sci. Technol.* **40**:357-
483 363.

484 Celiz MD, Tso J and Aga DS (2009) Pharmaceutical metabolites in the environment:
485 analytical challenges and ecological risks. *Environ. Toxicol. Chem.* **28**:2473-2484.

486 Chen L-J and Burka LT (2007) Chemical and Enzymatic Oxidation of Furosemide: Formation
487 of Pyridinium Salts. *Chem. Res. Toxicol.* **20**:1741-1744.

488 Daughton CG (2002) Environmental stewardship and drugs as pollutants. *Lancet* **360**:1035-
489 1036.

490 Daughton CG and Ternes TA (1999) Pharmaceuticals and personal care products in the
491 environment: agents of subtle change? *Environ. Health Perspect. Suppl.* **107**:907-938.

492 Deblonde T, Cossu-Leguille C and Hartemann P (2011) Emerging pollutants in wastewater: A
493 review of the literature. *Int. J. Hyg. Environ. Health* **214**:442-448.

494 Dirany A, Efremova Aaron S, Oturan N, Sires I, Oturan MA and Aaron JJ (2011) Study of the
495 toxicity of sulfamethoxazole and its degradation products in water by a
496 bioluminescence method during application of the electro-Fenton treatment. *Anal.*
497 *Bioanal. Chem.* **400**:353-360.

498 Dirany A, Sires I, Oturan N and Oturan MA (2010) Electrochemical abatement of the
499 antibiotic sulfamethoxazole from water. *Chemosphere* **81**:594-602.

500 Dirany A, Sires I, Oturan N, Ozcan A and Oturan MA (2012) Electrochemical wastewater
501 treatment for antibiotic sulfachloropyridazine degradation: kinetics, reaction pathways,
502 and toxicity evolution. *Environ. Sci. Technol.* **46**:4074-4082.

503 Ericson JF (2010) Evaluation of the OECD 314B Activated Sludge Die-Away Test for
504 Assessing the Biodegradation of Pharmaceuticals. *Environ. Sci. Technol.* **44**:375-381.

505 Escher BI and Fenner K (2011) Recent Advances in Environmental Risk Assessment of
506 Transformation Products. *Environ. Sci. Technol.* **45**:3835-3847.

507 Fatta-Kassinos D, Meric S and Nikolaou A (2011a) Pharmaceutical residues in environmental
508 waters and wastewater: current state of knowledge and future research. *Anal. Bioanal.*
509 *Chem.* **399**:251-275.

510 Fatta-Kassinos D, Vasquez MI and Kuemmerer K (2011b) Transformation products of
511 pharmaceuticals in surface waters and wastewater formed during photolysis and
512 advanced oxidation processes - Degradation, elucidation of byproducts and assessment
513 of their biological potency. *Chemosphere* **85**:693-709.

514 Fromentin Y, Grellier P, Wansi JD, Lallemand M-C and Buisson D (2012) Yeast-Mediated
515 Xanthone Synthesis through Oxidative Intramolecular Cyclization. *Org. Lett.*
516 **14**:5054-5057.

517 Gauthier H, Yargeau V and Cooper DG (2010) Biodegradation of pharmaceuticals by
518 *Rhodococcus rhodochrous* and *Aspergillus niger* by co-metabolism. *Sci. Total*
519 *Environ.* **408**:1701-1706.

520 Heberer T (2002) Occurrence, fate, and removal of pharmaceutical residues in the aquatic
521 environment: a review of recent research data. *Toxicol. Lett.* **131**:5-17.

522 Henschel KP, Wenzel A, Diedrich M and Fliedner A (1997) Environmental hazard
523 assessment of pharmaceuticals. *Regul. Toxicol. Pharmacol.* **25**:220-225.

524 Hezari M and Davis PJ (1992) Microbial models of mammalian metabolism. N-dealkylation
525 of furosemide to yield the mammalian metabolite CSA using *Cunninghamella elegans*.
526 *Drug Metab. Dispos.* **20**:882-888.

527 Ibanez M, Sancho JV, Pozo OJ and Hernandez F (2004) Use of Quadrupole Time-of-Flight
528 Mass Spectrometry in Environmental Analysis: Elucidation of Transformation
529 Products of Triazine Herbicides in Water after UV Exposure. *Anal. Chem.* **76**:1328-
530 1335.

531 Isidori M, Nardelli A, Parrella A, Pascarella L and Previtera L (2006) A multispecies study to
532 assess the toxic and genotoxic effect of pharmaceuticals: Furosemide and its
533 photoproduct. *Chemosphere* **63**:785-793.

534 Joyeau R, Planchon M, Abessolo J, Aissa K, Bance C and Buisson D (2013) Combinatorial
535 approach to the selection of active microorganisms in biotransformation: Application
536 to sinomenine. *J. Mol. Catal. B: Enzym.* **85-86**:65-70.

537 Jurado A, Vazquez-Sune E, Carrera J, Lopez de Alda M, Pujades E and Barcelo D (2012)
538 Emerging organic contaminants in groundwater in Spain: A review of sources, recent
539 occurrence and fate in a European context. *Sci. Total Environ.* **440**:82-94.

540 Khalaf H, Salste L, Karlsson P, Ivarsson P, Jass J and Olsson P-E (2009) In vitro analysis of
541 inflammatory responses following environmental exposure to pharmaceuticals and
542 inland waters. *Sci. Total Environ.* **407**:1452-1460.

543 Khetan SK and Collins TJ (2007) Human Pharmaceuticals in the Aquatic Environment: A
544 Challenge to Green Chemistry. *Chem. Rev. (Washington, DC, U. S.)* **107**:2319-2364.

545 Koopman F, Wierckx N, de WJH and Ruijssenaars HJ (2010) Identification and
546 characterization of the furfural and 5-(hydroxymethyl)furfural degradation pathways
547 of *Cupriavidus basilensis* HMF14. *Proc. Natl. Acad. Sci. U. S. A.* **107**:4919-4924,
548 S4919/4911-S4919/4915.

549 Kuemmerer KE (2004) *Pharmaceuticals in the Environment: Sources, Fate, Effects and*
550 *Risks, Second Edition.* Springer GmbH.

551 Laurence C, Rivard M, Lachaise I, Bensemhoun J and Martens T (2011) Preparative access to
552 transformation products (TPs) of furosemide: a versatile application of anodic
553 oxidation. *Tetrahedron* **67**:9518-9521.

554 Lee WI, Yoon WH, Shin WG, Song IS and Lee MG (1997) Pharmacokinetics and
555 pharmacodynamics of furosemide after direct administration into the stomach or
556 duodenum. *Biopharm. Drug Dispos.* **18**:753-767.

557 Levi Y (2009) Challenges in the assessment and management of health risks associated with
558 emerging water micropollutants. *Bull. Acad. Natl. Med. (Paris, Fr.)* **193**:1331-1344.

559 Li W, Josephs JL, Skiles GL and Humphreys WG (2008) Metabolite generation via microbial
560 biotransformations with actinomycetes: rapid screening for active strains and
561 biosynthesis of important human metabolites of two development-stage compounds,
562 5-[(5S,9R)-9-(4-cyanophenyl)-3-(3,5-dichlorophenyl)-1-methyl-2,4-dioxo-1,3,7-
563 triazaspiro[4.4]non-7-yl-methyl]-3-thiophenecarboxylic acid (BMS-587101) and
564 dasatinib. *Drug Metab. Dispos.* **36**:721-730.

565 Lohmann W and Karst U (2008) Biomimetic modeling of oxidative drug metabolism. *Anal.*
566 *Bioanal. Chem.* **391**:79-96.

- 567 Marvalin C and Azerad R (2011) Microbial production of phase I and phase II metabolites of
568 propranolol. *Xenobiotica* **41**:175-186.
- 569 Mompelat S, Le Bot B and Thomas O (2009) Occurrence and fate of pharmaceutical products
570 and by-products, from resource to drinking water. *Environ. Int.* **35**:803-814.
- 571 Mondal SC, Tripathi DN, Vikram A, Ramarao P and Jena GB (2012) Furosemide-induced
572 genotoxicity and cytotoxicity in the hepatocytes, but weak genotoxicity in the bone
573 marrow cells of mice. *Fundam. Clin. Pharmacol.* **26**:383-392.
- 574 Oturan MA, Peirotten J, Chartrin P and Acher AJ (2000) Complete Destruction of p-
575 Nitrophenol in Aqueous Medium by Electro-Fenton Method. *Environ. Sci. Technol.*
576 **34**:3474-3479.
- 577 Oturan MA, Pinson J, Oturan N and Deprez D (1999) Hydroxylation of aromatic drugs by the
578 electro-Fenton method. Formation and identification of the metabolites of Riluzole.
579 *New J. Chem.* **23**:793-794.
- 580 Ozcan A, Sahin Y, Koparal AS and Oturan MA (2008) Degradation of picloram by the
581 electro-Fenton process. *J Hazard Mater* **153**:718-727.
- 582 Packer JL, Werner JJ, Latch DE, McNeill K and Arnold WA (2003) Photochemical fate of
583 pharmaceuticals in the environment: naproxen, diclofenac, clofibric acid, and
584 ibuprofen. *Aquat. Sci.* **65**:342-351.
- 585 Rakonczay Z, Jr., Hegyi P, Hasegawa M, Inoue M, You J, Iida A, Ignath I, Alton EFWF,
586 Griesenbach U, Ovari G, Vag J, Da PAC, Crawford RM, Varga G, Amaral MD,
587 Mehta A, Lonovics J, Argent BE and Gray MA (2008) CFTR gene transfer to human
588 cystic fibrosis pancreatic duct cells using a Sendai virus vector. *J Cell Physiol*
589 **214**:442-455.
- 590 Richardson SD (2010) Environmental Mass Spectrometry: Emerging Contaminants and
591 Current Issues. *Anal. Chem. (Washington, DC, U. S.)* **82**:4742-4774.
- 592 Rocco L, Frenzilli G, Fusco D, Peluso C and Stingo V (2010) Evaluation of zebrafish DNA
593 integrity after exposure to pharmacological agents present in aquatic environments.
594 *Ecotoxicol. Environ. Saf.* **73**:1530-1536.
- 595 Rodil R, Quintana JB, Concha-Grana E, Lopez-Mahia P, Muniategui-Lorenzo S and Prada-
596 Rodriguez D (2012) Emerging pollutants in sewage, surface and drinking water in
597 Galicia (NW Spain). *Chemosphere* **86**:1040-1049.
- 598 Schulze T, Weiss S, Schymanski E, von der Ohe PC, Schmitt-Jansen M, Altenburger R,
599 Streck G and Brack W (2010) Identification of a phytotoxic photo-transformation

600 product of diclofenac using effect-directed analysis. *Environ. Pollut. (Oxford, U. K.)*
601 **158**:1461-1466.

602 Sires I, Garrido JA, Rodriguez RM, Brillas E, Oturan N and Oturan MA (2007) Catalytic
603 behavior of the Fe³⁺/Fe²⁺ system in the electro-Fenton degradation of the
604 antimicrobial chlorophene. *Appl. Catal., B* **72**:382-394.

605 Sires I, Oturan N and Oturan MA (2010) Electrochemical degradation of β -blockers. Studies
606 on single and multicomponent synthetic aqueous solutions. *Water Res.* **44**:3109-3120.

607 Smith RV and Rosazza JP (1975) Microbial models of mammalian metabolism. *J. Pharm.*
608 *Sci.* **64**:1737-1759.

609 Svanfelt J and Kronberg L (2011) Synthesis of substituted diphenylamines and carbazoles:
610 phototransformation products of diclofenac. *Environ. Chem. Lett.* **9**:141-144.

611 Wierckx N, Koopman F, Ruijsenaars HJ and Winde JH (2011) Microbial degradation of
612 furanic compounds: biochemistry, genetics, and impact. *Appl. Microbiol. Biotechnol.*
613 **92**:1095-1105.

614 Williams DP, Antoine DJ, Butler PJ, Jones R, Randle L, Payne A, Howard M, Gardner I,
615 Blagg J and Park BK (2007) The metabolism and toxicity of furosemide in the Wistar
616 rat and CD-1 mouse: a chemical and biochemical definition of the toxicophore. *J.*
617 *Pharmacol. Exp. Ther.* **322**:1208-1220.

618 Ziylan A and Ince NH (2011) The occurrence and fate of anti-inflammatory and analgesic
619 pharmaceuticals in sewage and fresh water: Treatability by conventional and non-
620 conventional processes. *J. Hazard. Mater.* **187**:24-36.

621
622

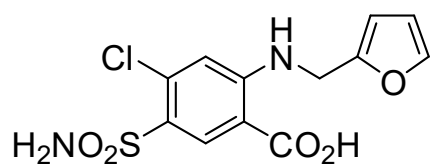
Figure captions

Figure 1: Furosemide 1 and its TPs

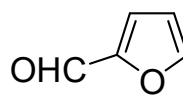
Figure 2: Structures proposed for a) m/z 345, b) m/z 317 and 282

Figure 3: Cytotoxic evaluation of pyridinium 4. A) Concentration-dependant survival of neuroblastoma cells (SH-SY5Y) exposed for 96 h to pyridinium 4. Percentage survival was calculated using values obtained for untreated cells in the MTT assays as a reference. The calculated EC_{50} was $973 \pm 46 \mu\text{M}$. B) The caspase-3 activity was measured after 96 h of treatment with pyridinium 4 (1 mM). Data shown are the mean \pm S.E.M. of 3 independent experiments with duplicate wells per experiment, * $p < 0.05$ compared with control.

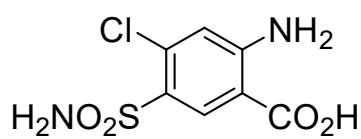
Figure 1



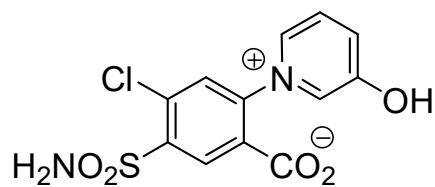
1



2



3



4

Figure 2

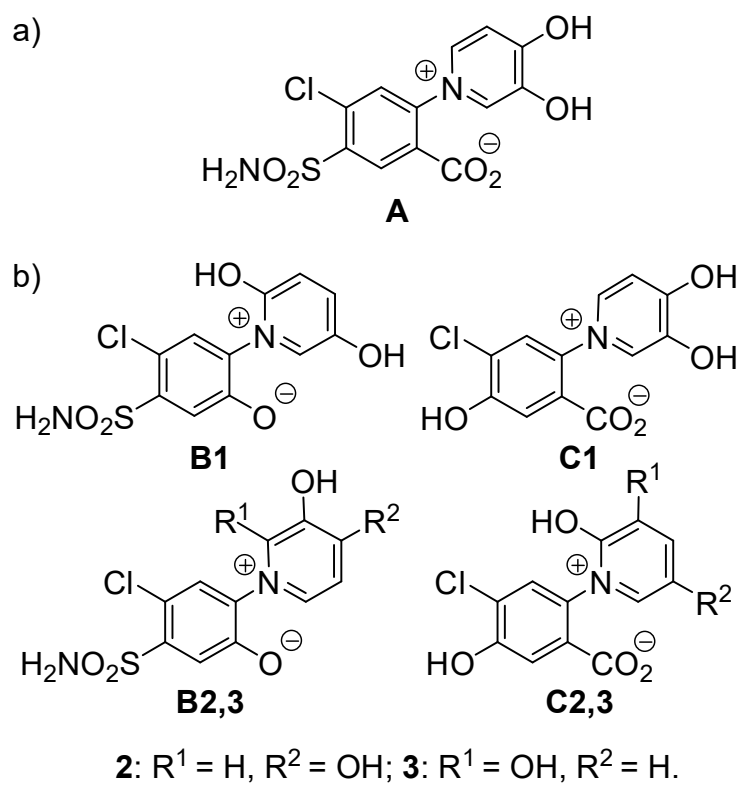
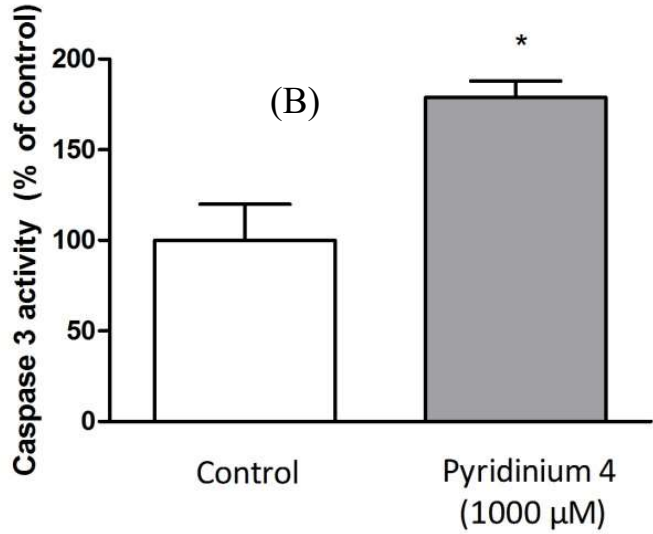
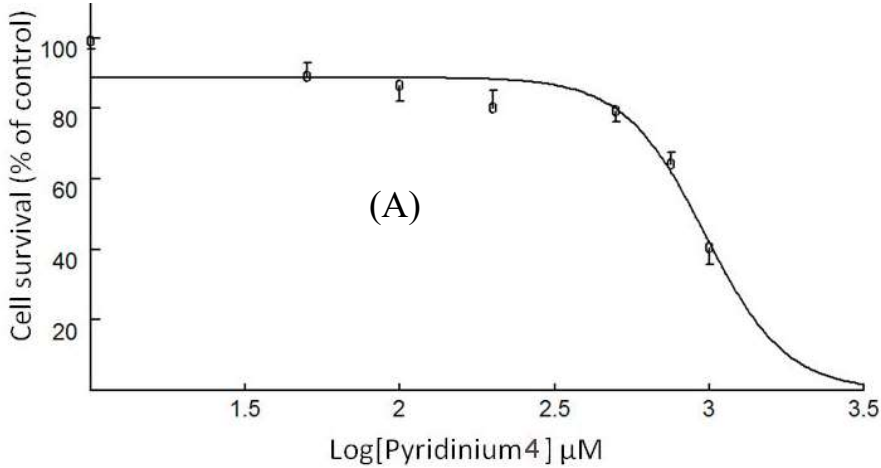


Figure 3



Supplementary Materials

Anticipating the Fate and Impact of Organic Environmental Contaminants: a New Approach Applied to the Pharmaceutical Furosemide.

Céline Laurencé,^a Michael Rivard,^a Thierry Martens,^{a,} Christophe Morin,^b Didier Buisson,^c Sophie Bourcier,^d Michel Sablier^{d,e} and Mehmet A. Oturan^{f,*}*

^aUniversité Paris-Est, Institut de Chimie et des Matériaux de Paris-Est
UMR CNRS UPEC 7182 - 94320 Thiais, France

^bUniversité Paris-Est, Laboratoire Croissance Réparation et Régénération Tissulaires
EAC CNRS 7149 - UPEC, 94010 Créteil cedex, France

^cMuséum National d'Histoire Naturelle, Unité Molécules de Communication et
Adaptation des Microorganismes, UMR CNRS MNHM 7245 - 75005 Paris, France

^dEcole Polytechnique, Laboratoire des Mécanismes Réactionnels
UMR CNRS Ecole Polytechnique 7651 - 91128 Palaiseau cedex, France

^eMuséum National d'Histoire Naturelle, Centre de Recherche sur la Conservation des
Collections, USR CNRS MNHN 3224 - 75005 Paris, France

^fUniversité Paris-Est, Laboratoire Géomatériaux et Environnement, EA 4508
UPEMLV, 77454 Marne-la-Vallée, France

* Corresponding authors:

Mehmet A. Oturan

Email: mehmet.oturan@univ-paris-est.fr

Phone: +33 (0)1 49 32 90 65

Fax: +33(0)1 49 32 91 37

Thierry Martens

Email: martens@icmpe.cnrs.fr

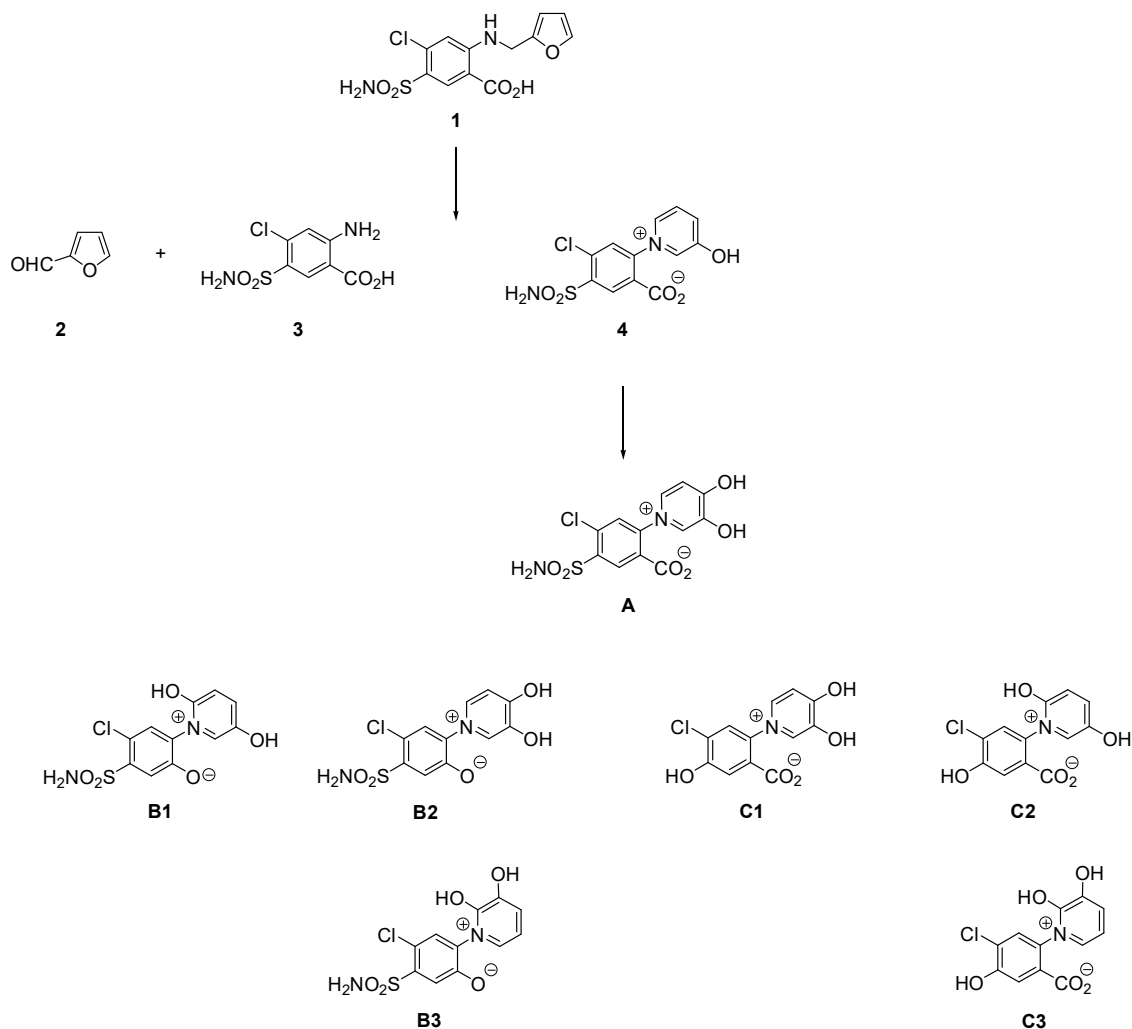
Phone: +33 (0)1 49 78 11 56

Fax: +33 (0)1 49 78 11 48

Table of contents

| | |
|--|----|
| 1. Furosemide 1 and its oxidation products | 28 |
| 2. Detection of 3 after electro-Fenton oxidation of 1 | 30 |
| 3. Detection of 3 after electro-Fenton oxidation of 4 | 30 |
| 4. Detection of 4 after electro-Fenton oxidation and bioconversion of 1 | 31 |
| 5. Detection of A after electro-Fenton oxidation and bioconversion of 1 and electro-Fenton oxidation of 4 | 33 |
| 6. Discussion on the structure of m/z 345, RT=5.24 min | 34 |
| 6.1 Expected fragmentations of MH ⁺ deriving from A | 34 |
| 6.2 Expected fragmentations of MH ⁺ deriving from A2 | 34 |
| 6.3 Expected fragmentations of MH ⁺ deriving from A3 | 35 |
| 6.4 Expected fragmentations of MH ⁺ deriving from A4 | 35 |
| 6.5 Expected fragmentations of MH ⁺ deriving from A5 | 36 |
| 7. Detection of B1 and B2 or C3 after electro-Fenton oxidation of 1 and 4 | 37 |
| 8. Discussion on the structures of m/z 317, RT=4.0 and 7.0 min | 37 |
| 8.1 Expected fragmentations of MH ⁺ deriving from B1 | 38 |
| 8.2 Expected fragmentations of MH ⁺ deriving from B2 | 38 |
| 8.3 Expected fragmentations of MH ⁺ deriving from B3 | 39 |
| 8.4 Expected fragmentations of MH ⁺ deriving from B4 | 39 |
| 8.5 Expected fragmentations of MH ⁺ deriving from B5 | 40 |
| 9. Detection of C1 and C2 or C3 after electro-Fenton oxidation and bioconversion of 1 and electro-Fenton oxidation of 4 | 40 |
| 10. Discussion on the structures of m/z 282, RT=4.2 and 10.4 min | 41 |
| 10.1 Expected fragmentations of MH ⁺ deriving from C1 | 42 |
| 10.2 Expected fragmentations of MH ⁺ deriving from C2 | 42 |
| 10.3 Expected fragmentations of MH ⁺ deriving from C3 | 42 |
| 10.4 Expected fragmentations of MH ⁺ deriving from C4 | 43 |
| 10.5 Expected fragmentations of MH ⁺ deriving from C5 | 43 |

1. Furoseamide **1** and its oxidation products



| Oxidation products | Retention Time (min) | Molecular Weight (m/z) | Experimental Mass | Theoretical Mass | m/z | p | D BE ¹ | Elemental composition | Detection | | |
|--------------------|----------------------|------------------------|-------------------|------------------|-----|-----|-------------------|--|-----------|----|----|
| | | | | | | | | | a) | b) | c) |
| 3 | 5.2 | 251 | 250. | 250. | 1.3 | 5.2 | 4.5 | C ₇ H ₈ ClN ₂ O ₄ S | | | |
| | | | | | | | | | | | |
| 4 | 2.2 | 329 | 328. | 328. | 0 | 0 | 8.5 | C ₁₂ H ₁₀ ClN 2O ₅ S | | | |
| | | | | | | | | | | | |
| A | 5.24 | 349 | 344. | 344. | 0 | 0 | 8.5 | C ₁₂ H ₁₀ ClN 2O ₆ S | | | |
| | | | | | | | | | | | |
| B1 | 7 | 317 | 317. | 317. | - | - | 7 | C ₁₁ H ₁₀ ClN | | | |

| | | | | | | | | |
|-------------|-----|----|------|------|-----|-----|----|--|
| | .0 | 17 | 0005 | 0024 | 1.9 | 6 | .5 | $_2\text{O}_5\text{S}$ |
| B2or | 4 | 3 | 316. | 317. | - | - | 7 | $\text{C}_{11}\text{H}_{10}\text{ClN}$ |
| 3 | .0 | 17 | 9997 | 9999 | 0.2 | 0.6 | .5 | $_2\text{O}_5\text{S}$ |
| C1 | 1 | 2 | 282. | 282. | 0 | 2 | 8 | $\text{C}_{12}\text{H}_9\text{ClN}$ |
| | 0.4 | 82 | 0176 | 0169 | .7 | .5 | .5 | O_5 |
| C2or | 4 | 2 | 282. | 282. | - | - | 8 | $\text{C}_{12}\text{H}_9\text{ClN}$ |
| 3 | .2 | 82 | 0168 | 0169 | 0.1 | 0.4 | .5 | O_5 |

¹DBE: Double Bond Equivalency. ²Detection (+) during: (a) electro-Fenton oxidation of furosemide **1**, (b) electro-Fenton oxidation of pyridinium **4**, (c) bioconversion of furosemide **1**.

2. Detection of **3** after electro-Fenton oxidation of **1**

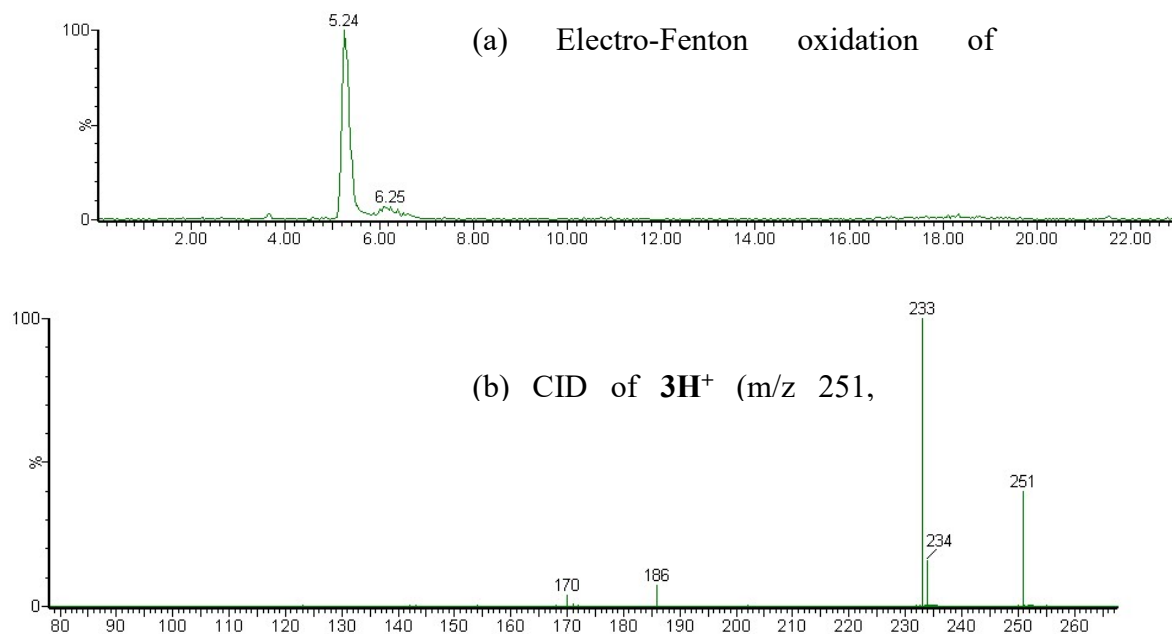
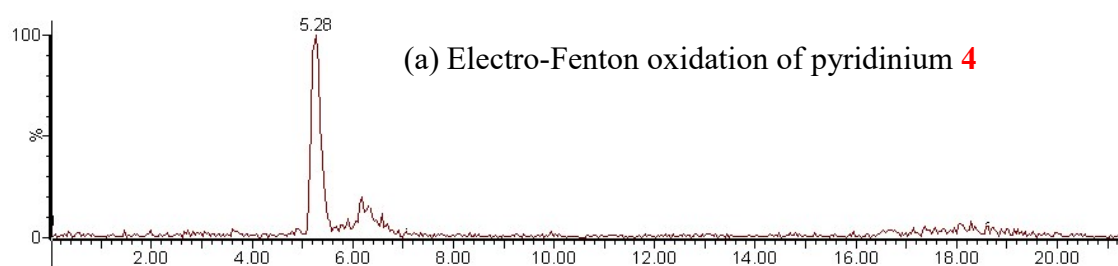


Fig. SM-1. (a) Extracted ion chromatogram (positive ion current) of m/z 251 for electro-Fenton oxidation of furosemide **1**. (b) CID mass spectrum of protonated molecular ion of compound **3** (MH^+ m/z 251), cone =25 V, Ecol = 10 eV. The CID spectrum of the ion at m/z 251 (RT=5.2 min) is the same as that obtained for the MH^+ of compound **3**.

3. Detection of **3** after electro-Fenton oxidation of **4**



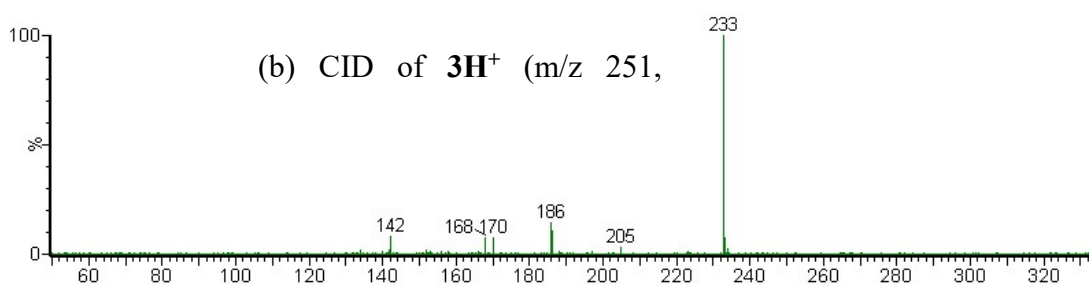


Fig. SM-2. (a) Extracted ion chromatogram (positive ion current) of m/z 251 for electro-Fenton oxidation of pyridinium **4**. (b) CID mass spectra of ion at m/z 251 at $\text{RT}=5.2$ min. Cone=25 V, $E_{\text{col}} = 15$ eV.

4. Detection of **4** after electro-Fenton oxidation and bioconversion of **1**

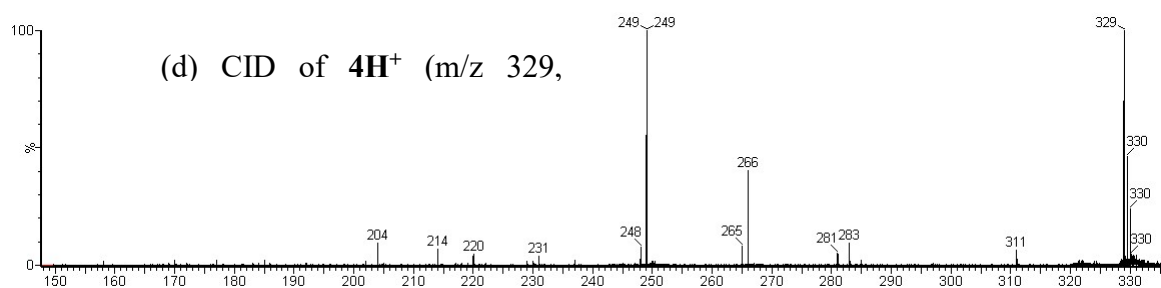
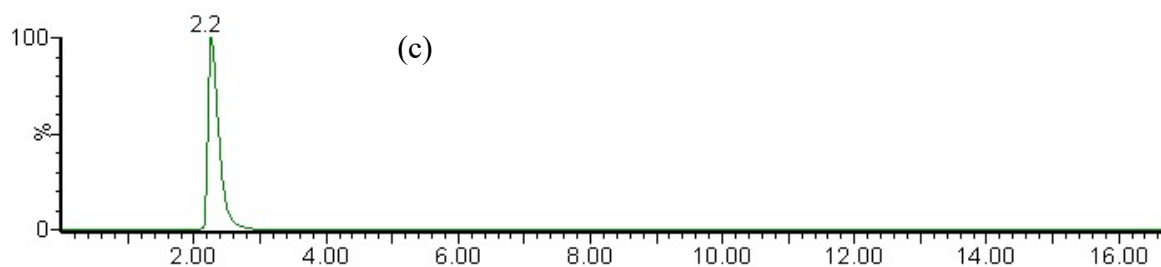
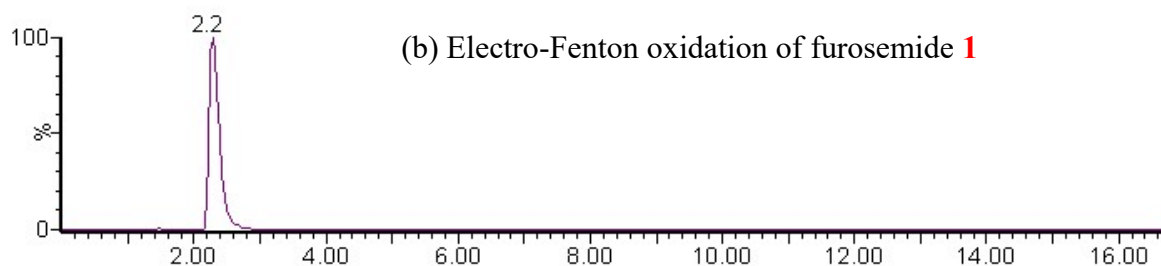
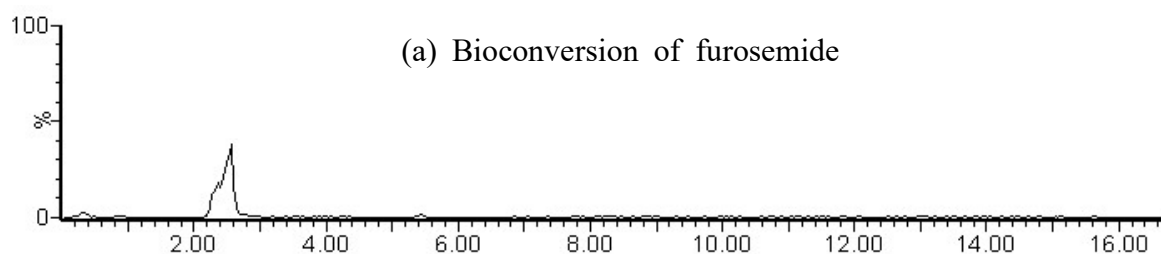


Fig. SM-3. Extracted ion chromatograms (positive ion current) of m/z 329 for (a), (b) and (c) samples. (d) CID mass spectrum of m/z 329 ion at $RT=2.2$ min. Cone =25 V, $E_{col}=10$ eV. This CID mass spectrum is the same for both samples (a) and (b) and corresponds to that of the pyridinium **4**.

5. Detection of A after electro-Fenton oxidation and bioconversion of **1** and electro-Fenton oxidation of **4**

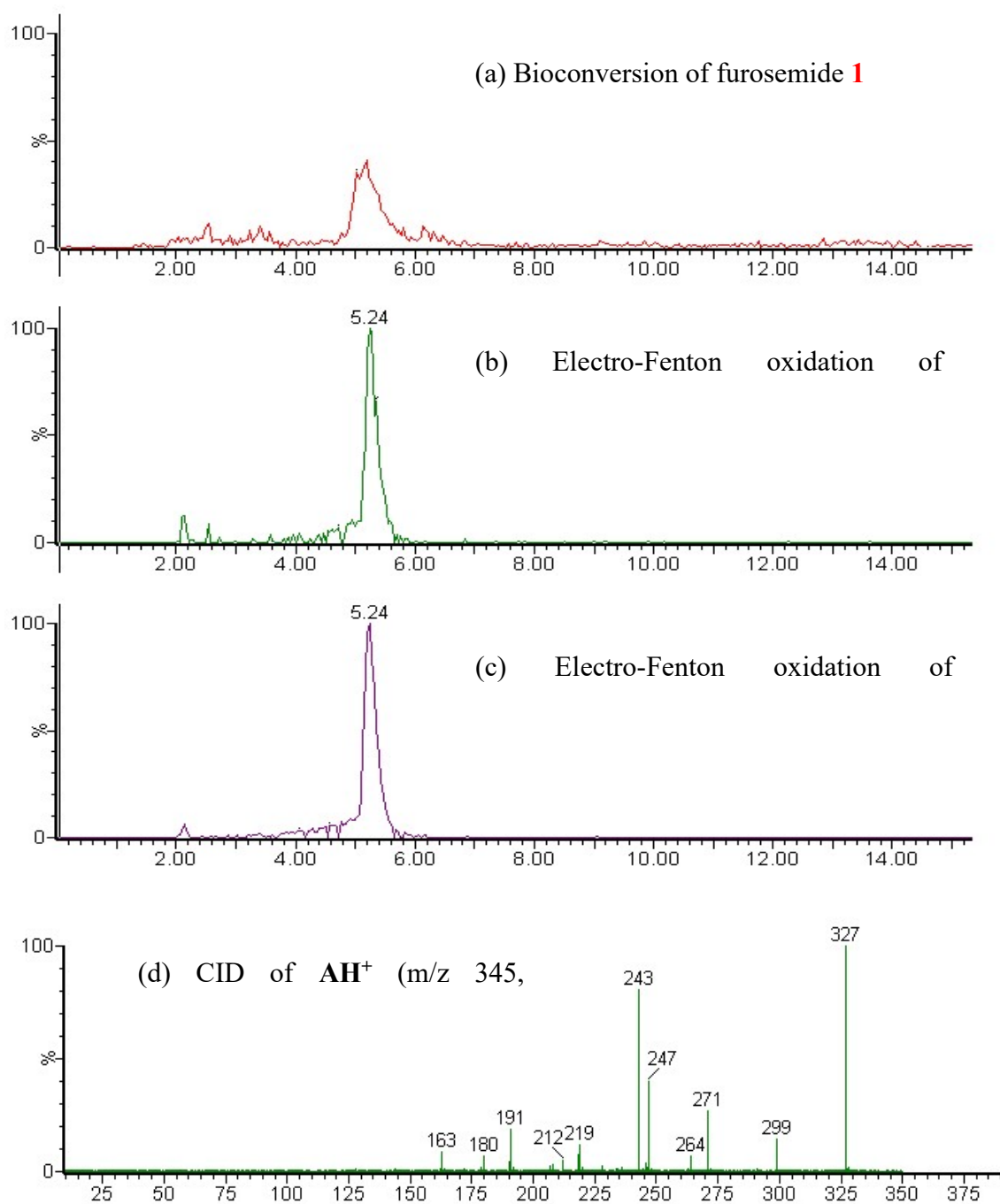
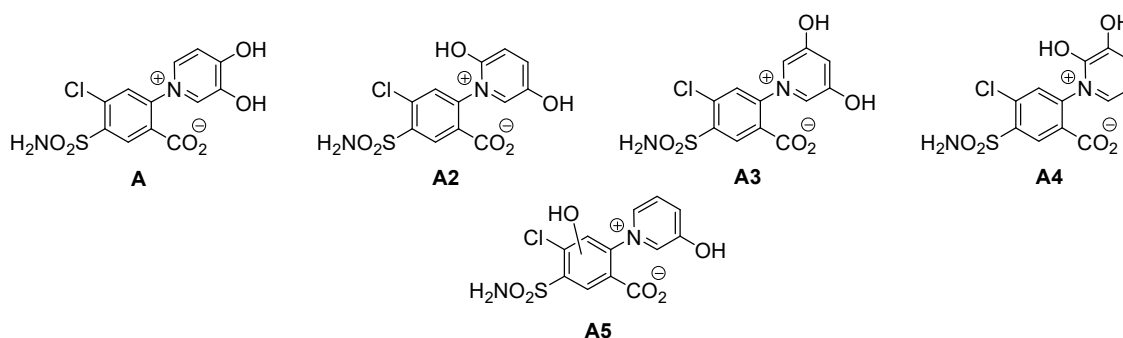


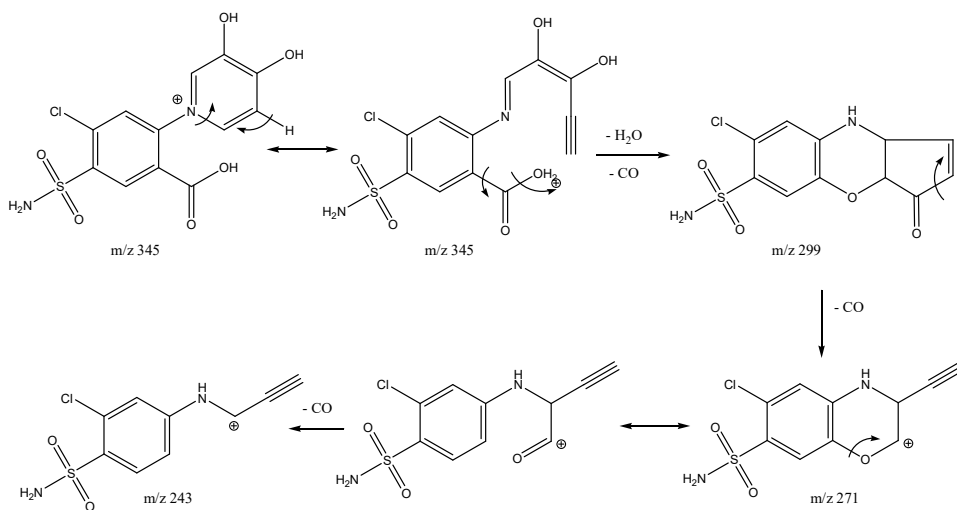
Fig. SM-4. Extracted ion chromatograms (positive ion current) of m/z 345 for (a), (b) and (c) samples. (d) CID mass spectra of MH^+ of compounds at m/z 345 (at $RT=5.24$ min). Cone=25 V, Ecol=15 eV. The selection of MH^+ is made only on ^{35}Cl isotope atom. Ions at m/z 327, 299, 271, 243 have preserved chlorine atom.

6. Discussion on the structure of m/z 345, $RT=5.24$ min

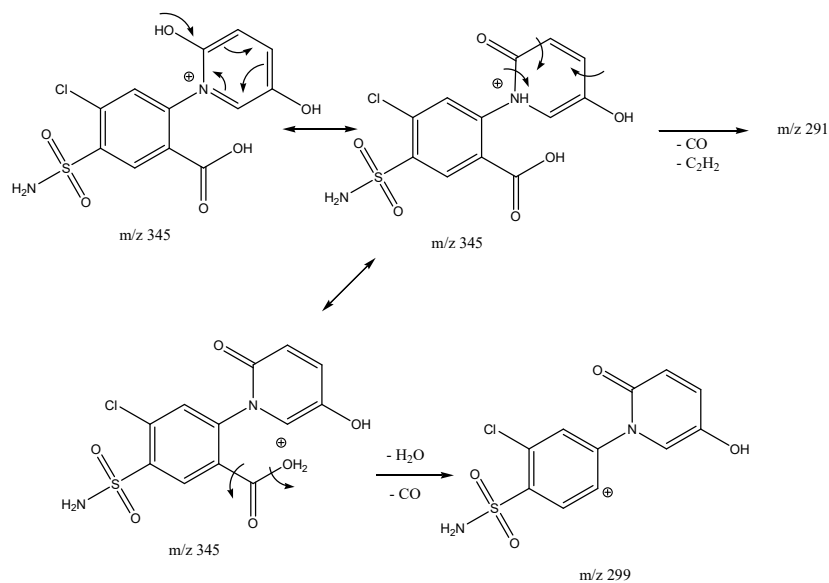
The elemental composition of the protonated molecular ion, eluted at $RT=5.24$ min, is $C_{12}H_{10}ClN_2O_6S$. This compound is corresponding to an oxidized form of pyridinium **4**. The protonated molecular ion loses one water molecule and one, two or three molecules of carbon monoxide to give ions at m/z 299, m/z 271 or m/z 243 respectively. Among the five possible structures **A**, **A2**, **A3**, **A4** and **A5**, only **A** revealed to be in agreement with the fragmentations observed.



6.1 Expected fragmentations of MH^+ deriving from **A**

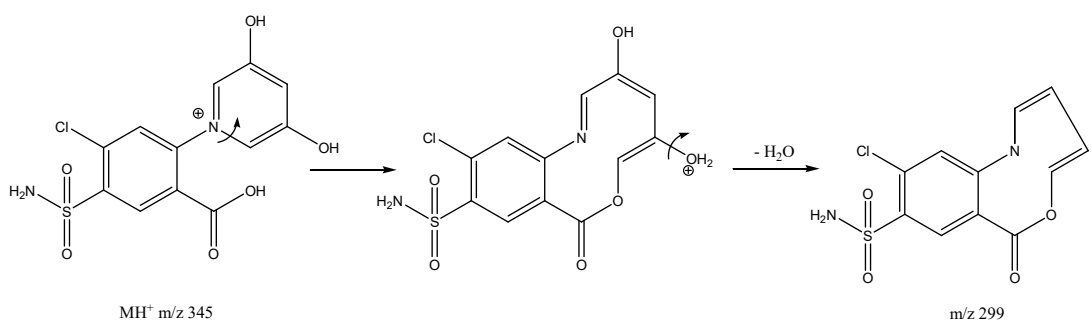


6.2 Expected fragmentations of MH^+ deriving from **A2**



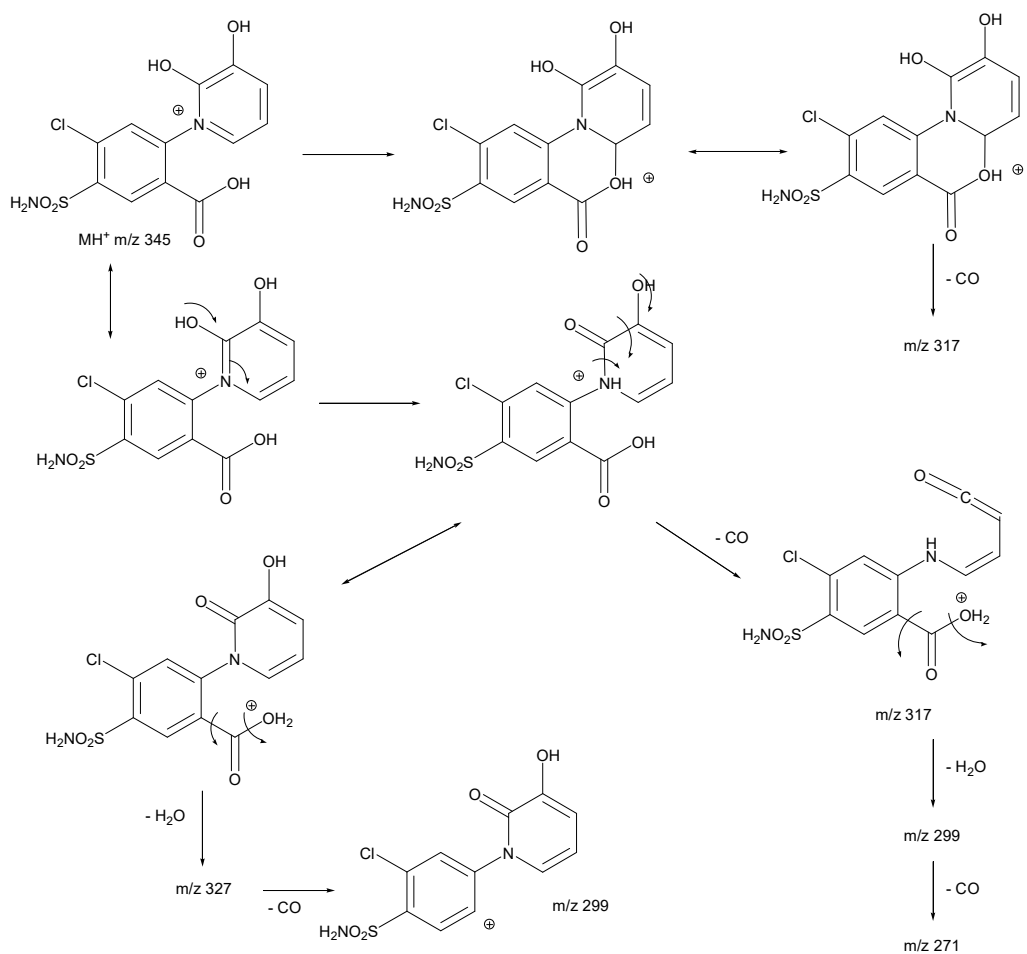
Ion at m/z 291 is not observed and m/z 299 does not allow the formation of ions observed at m/z 271 and m/z 243.

6.3 Expected fragmentations of MH^+ deriving from A3



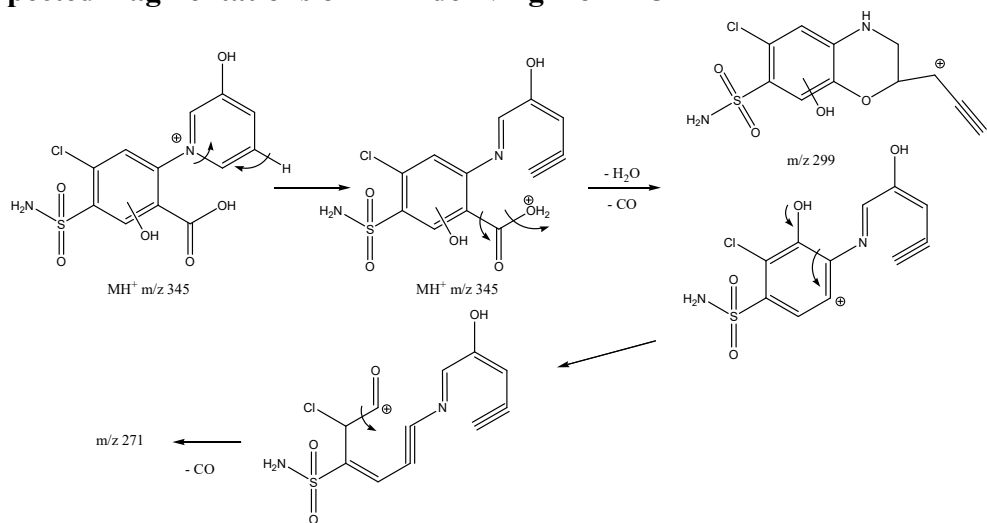
Ion at m/z 299 does not allow the formation of ion m/z 271.

6.4 Expected fragmentations of MH^+ deriving from A4



Ions at m/z 299 and m/z 271 do not allow the formation of ion at m/z 243. Ion at m/z 317 is not observed.

6.5 Expected fragmentations of MH^+ deriving from A5



Ion at m/z 271 does not allow the formation of ion at m/z 243.

7. Detection of B1 and B2 or B3 after electro-Fenton oxidation of **1** and **4**

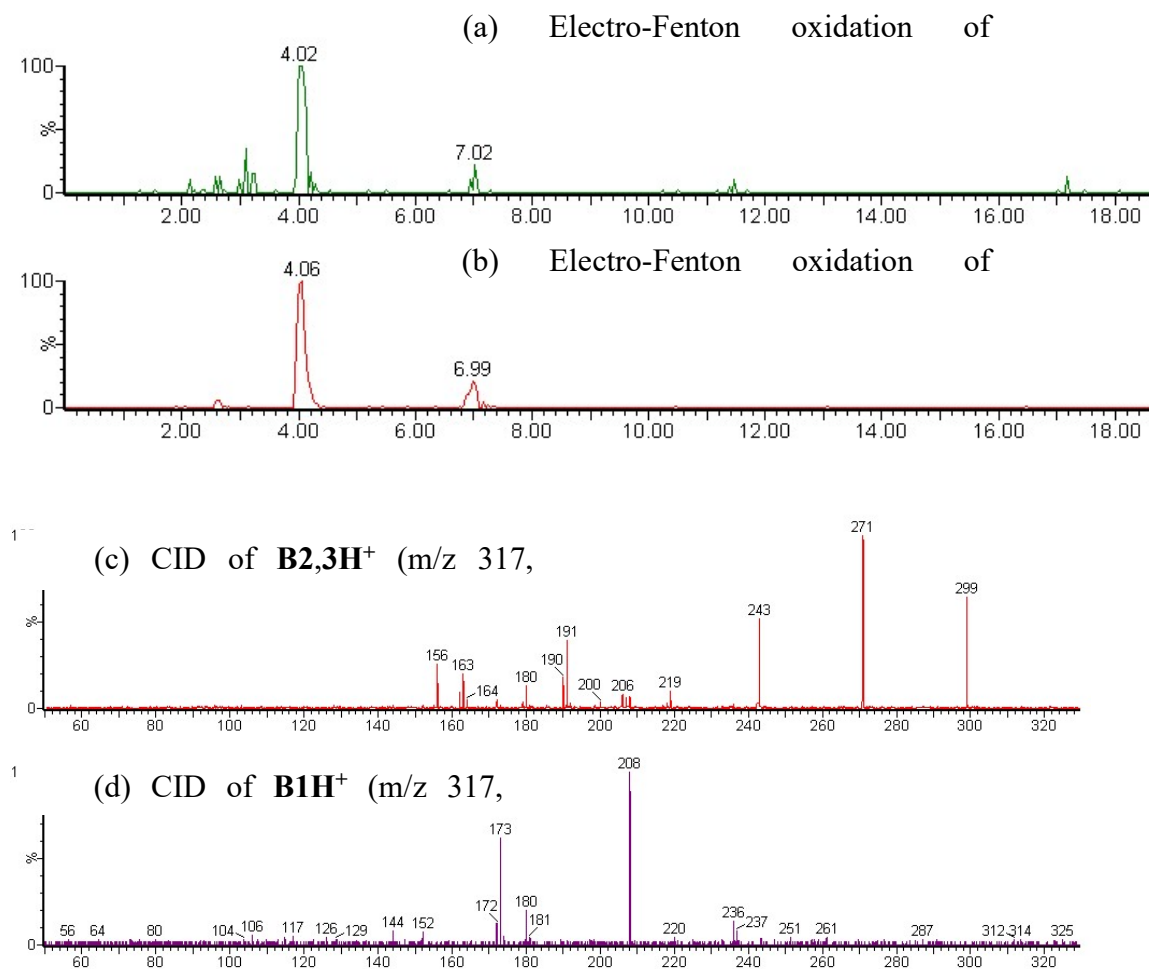
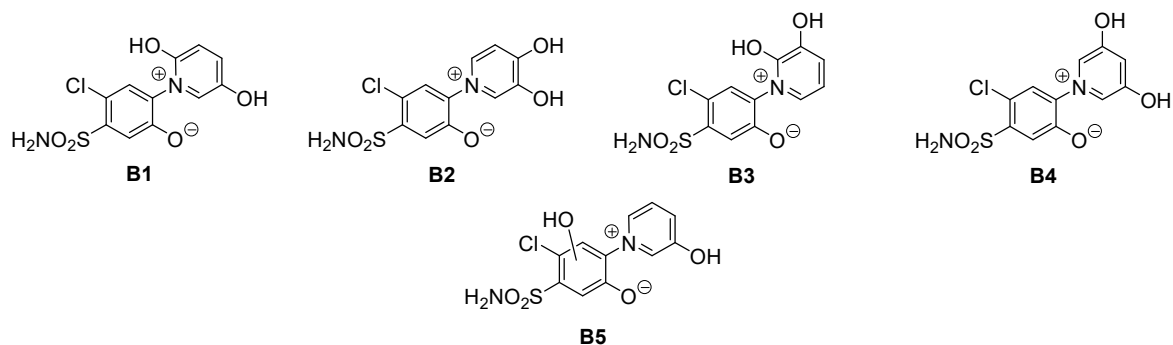


Fig. SM-5. Extracted ion chromatograms (positive ion current) of m/z 317 for electro-Fenton oxidation of (a) furosemide **1** and (b) electro-Fenton oxidation of pyridinium **4**. CID mass spectra of ion at m/z 317 at (c) RT=4.0 min and (d) RT=7.0 min. Cone=25 V, Ecol=15 eV.

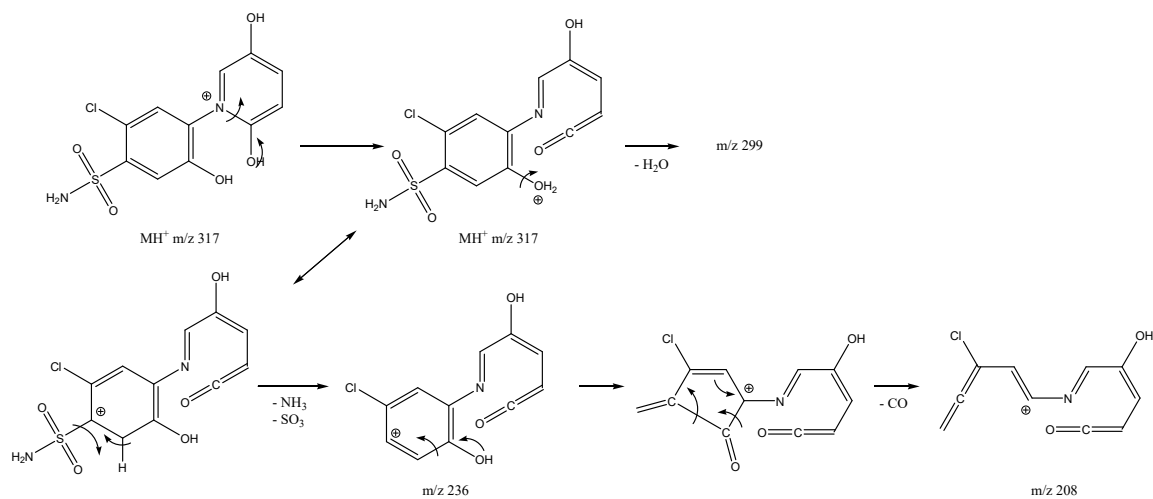
8. Discussion on the structures of m/z 317, RT=4.0 and 7.0 min

The elemental composition of both protonated molecular ions at m/z 317 is $C_{11}H_{10}ClN_2O_5S$. They lost a carbon and an oxygen atom relative to the pyridinium **4**. We assume that the CO of carboxylic function was lost. Five structures **B1**, **B2**, **B3**, **B4** and **B5** have been considered. **B1** is in agreement with the CID mass spectrum of MH^+ obtained for

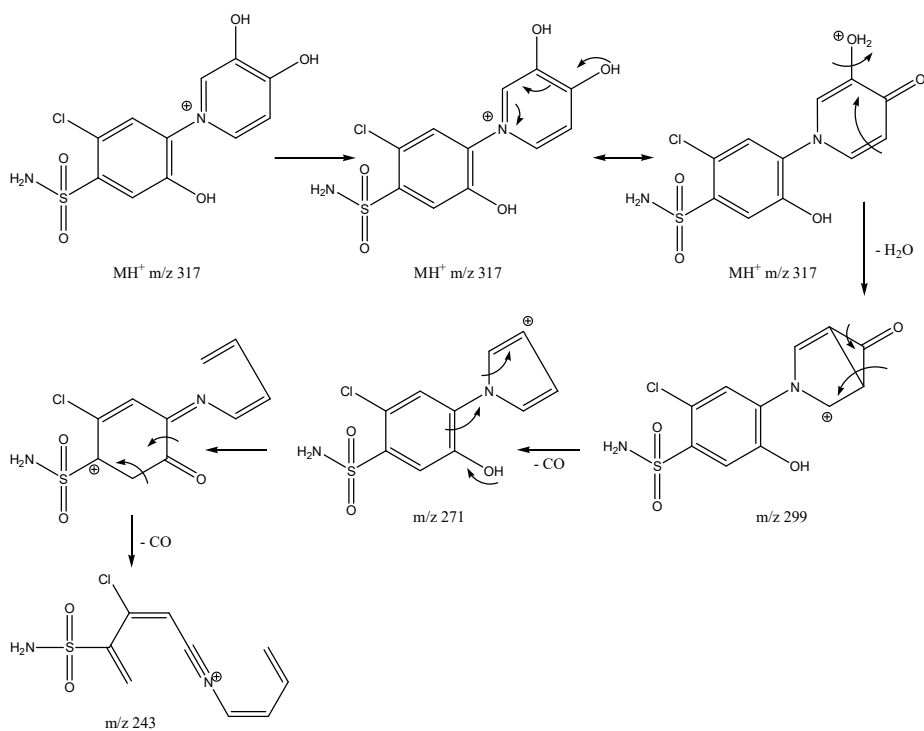
the compound eluted at 7 min. **B2** and **B3** both allow the formation of ions observed for the decomposition of MH^+ eluted at 4.0 min.



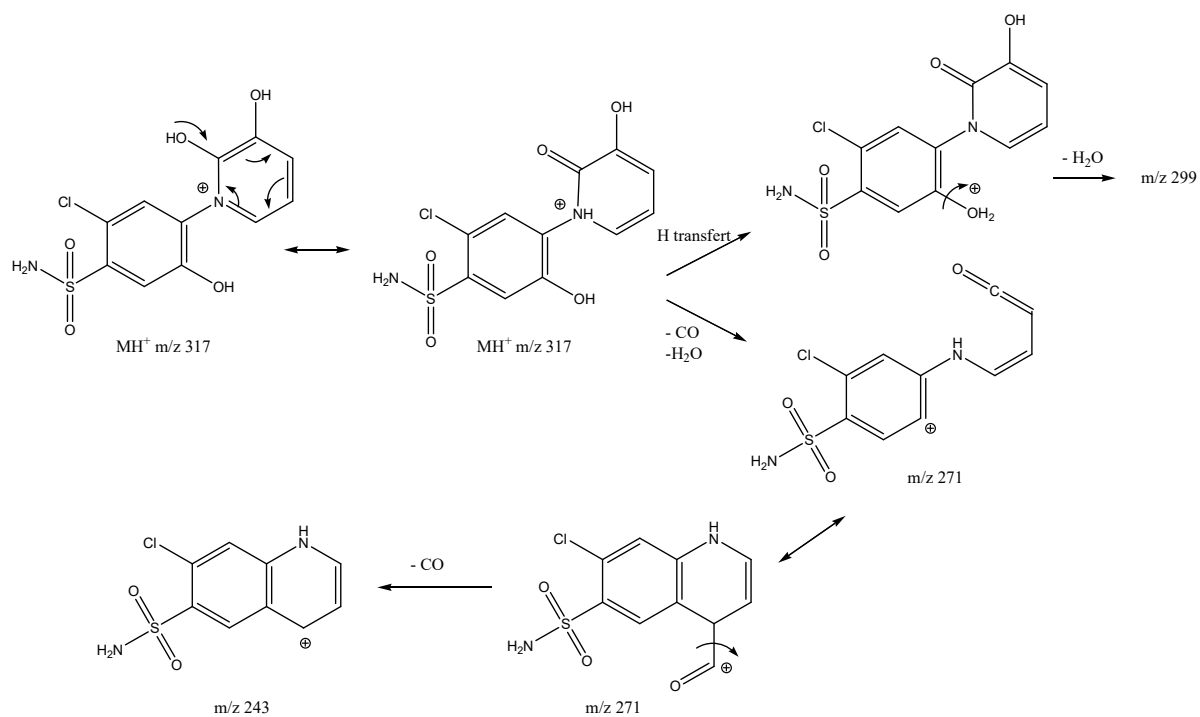
8.1 Expected fragmentations of MH^+ deriving from B1



8.2 Expected fragmentations of MH^+ deriving from B2



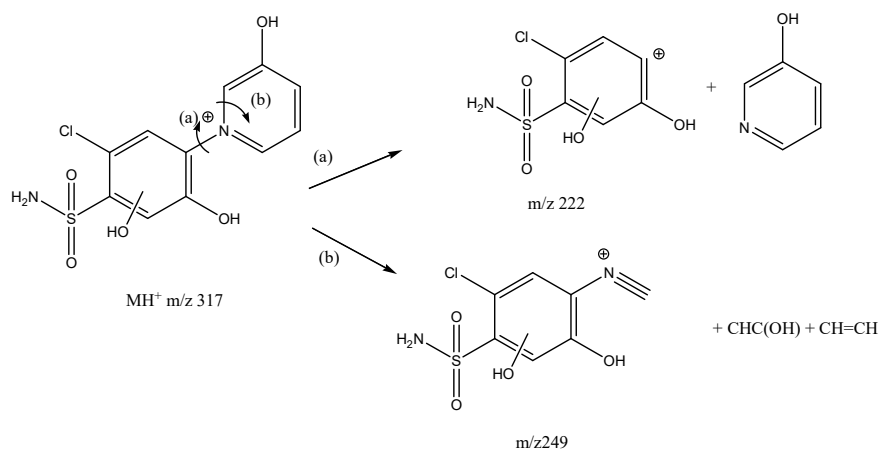
8.3 Expected fragmentations of MH^+ deriving from B3



8.4 Expected fragmentations of MH^+ deriving from B4

The fragmentation of **B4H⁺** leads to the elimination of one or two molecules of CHCOH to form the ions at m/z 275 and m/z 233 respectively. These ions are unobserved on CID mass spectra of m/z 317 (see 10.3).

8.5 Expected fragmentations of MH^+ deriving from **B5**



The proposed fragmentation of **B5H⁺** leads to the formation of two ions unobserved on CID mass spectra of m/z 317.

9. Detection of C1 and C2 or C3 after electro-Fenton oxidation and bioconversion of **1** and electro-Fenton oxidation of **4**

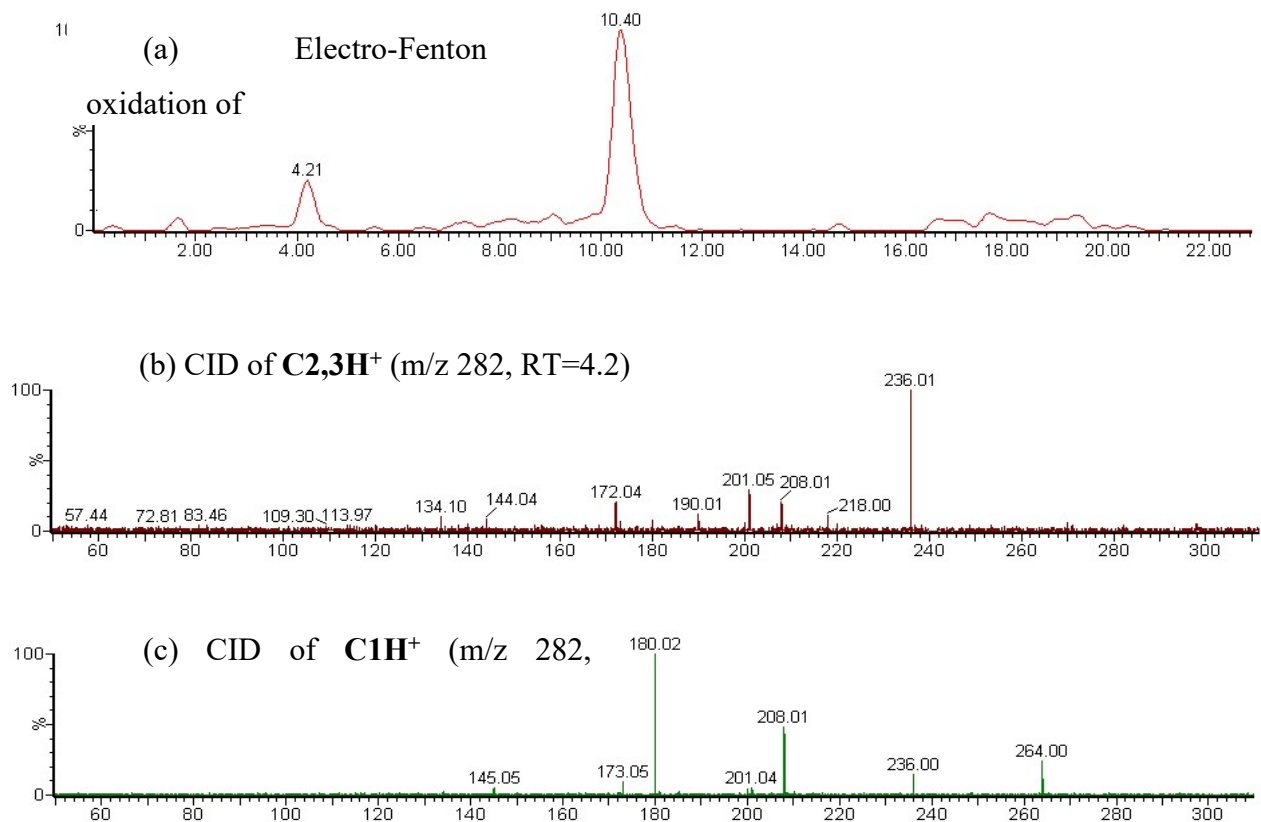
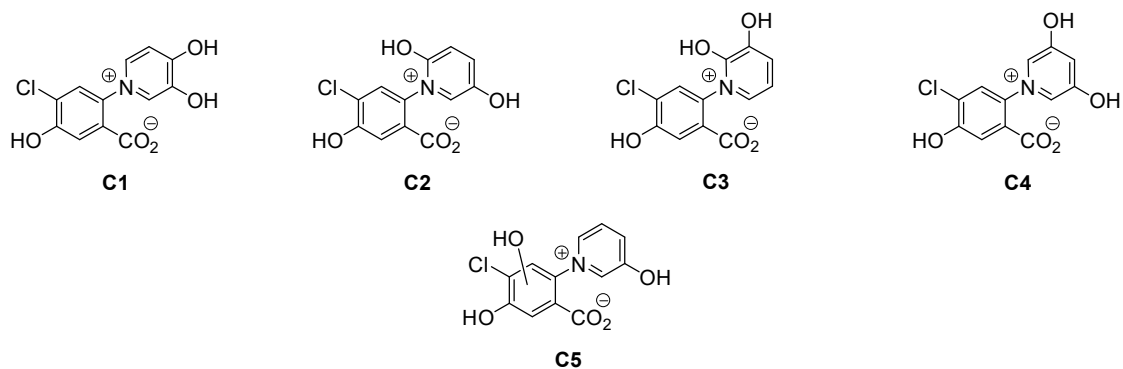


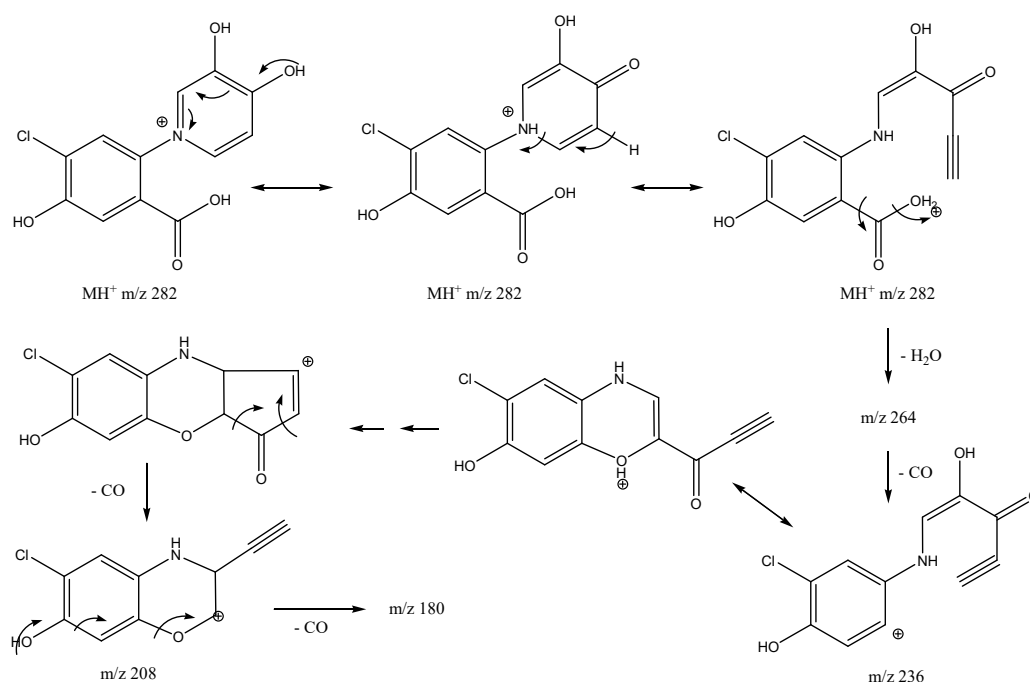
Fig. SM-6. (a) Extracted ion chromatogram (positive ion current) of m/z 282 for electro-Fenton oxidation of pyridinium **4**. CID mass spectra of ion at m/z 282 at (b) $RT=4.2$ min and (c) $RT=10.4$ min. Cone=25 V, Ecol=15 eV.

10. Discussion on the structures of m/z 282, $RT=4.2$ and 10.4 min

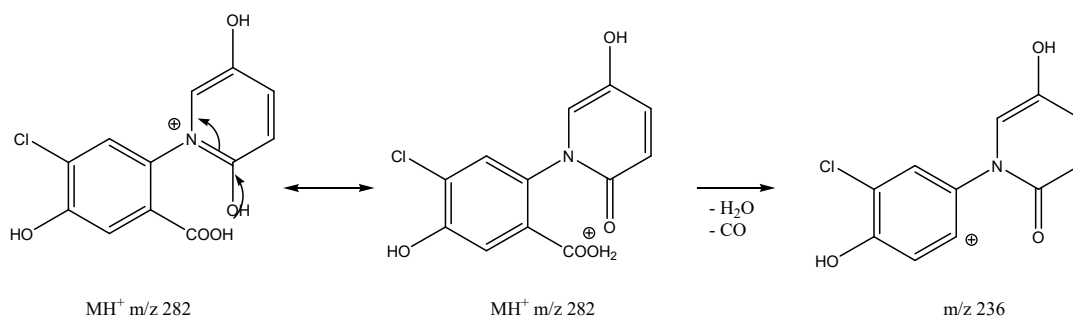
Structural characterization led to focus on the five compounds **C1**, **C2**, **C3**, **C4** and **C5**. **C1** is in agreement with fragmentations observed for $RT = 10.4$ min. Structures **C2** and **C3** both allow the formation of ions observed for the decomposition of MH^+ eluted at 4.2 min.



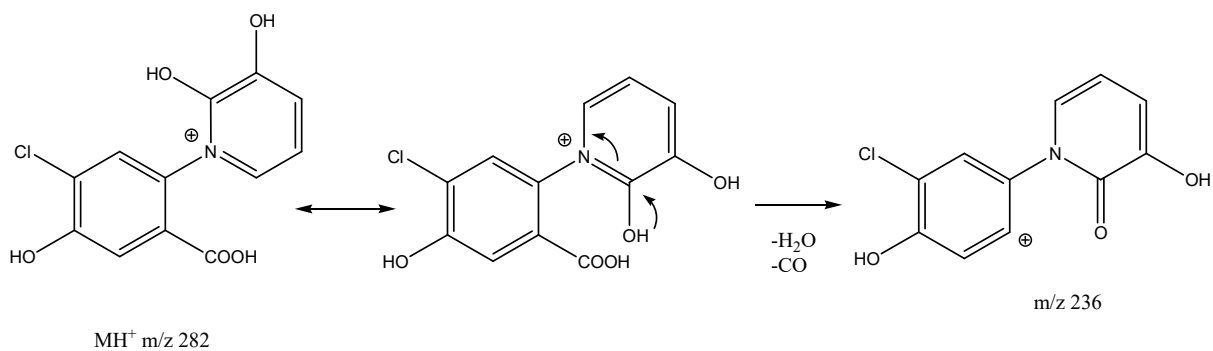
10.1 Expected fragmentations of MH⁺ deriving from C1



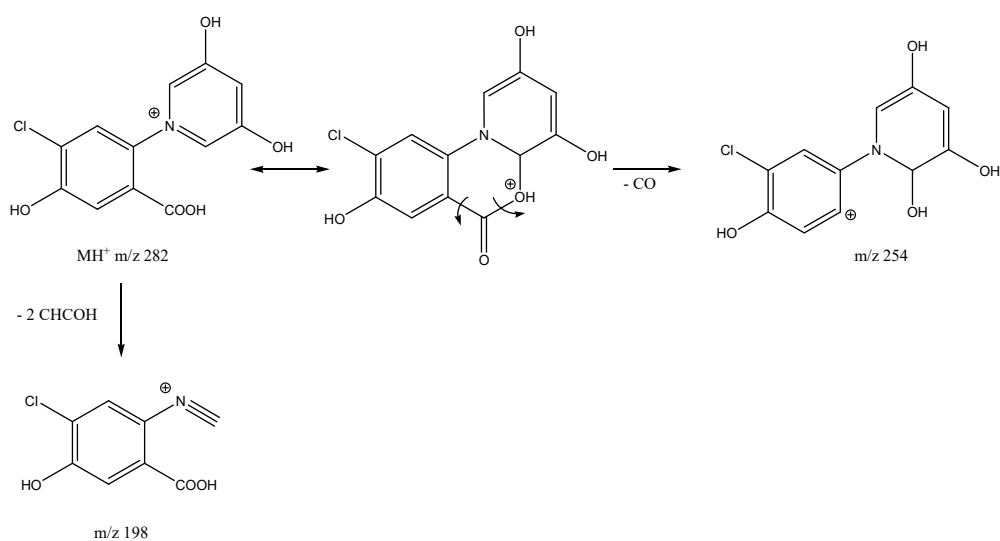
10.2 Expected fragmentations of MH⁺ deriving from C2



10.3 Expected fragmentations of MH⁺ deriving from C3



10.4 Expected fragmentations of MH^+ deriving from C4



The fragmentation of C4H^+ leads to the ions at $\text{m/z } 254$ and $\text{m/z } 198$ unobserved on CID mass spectra of $\text{m/z } 282$.

10.5 Expected fragmentations of MH^+ deriving from C5

